World Journal of Gastroenterology

Submit a Manuscript: https://www.f6publishing.com

World J Gastroenterol 2022 March 14; 28(10): 1024-1054

DOI: 10.3748/wjg.v28.i10.1024

ISSN 1007-9327 (print) ISSN 2219-2840 (online)

ORIGINAL ARTICLE

Basic Study

Loss of LAT1 sex-dependently delays recovery after caerulein-induced acute pancreatitis

Cristina M Hagen, Eva Roth, Theresia Reding Graf, François Verrey, Rolf Graf, Anurag Gupta, Giovanni Pellegrini, Nadège Poncet, Simone Mafalda Rodrigues Camargo

Specialty type: Gastroenterology and hepatology

Provenance and peer review: Unsolicited article; Externally peer reviewed.

Peer-review model: Single blind

Peer-review report's scientific quality classification
Grade A (Excellent): A
Grade B (Very good): 0
Grade C (Good): 0
Grade D (Fair): 0
Grade E (Poor): 0

P-Reviewer: Zharikov YO

Received: August 22, 2021
Peer-review started: August 22, 2021
First decision: September 12, 2021
Revised: October 8, 2021
Accepted: January 27, 2022
Article in press: January 27, 2022
Published online: March 14, 2022

Cristina M Hagen, Eva Roth, François Verrey, Nadège Poncet, Simone Mafalda Rodrigues Camargo, Institute of Physiology, University of Zurich, Zurich 8057, ZH, Switzerland

Theresia Reding Graf, Rolf Graf, Anurag Gupta, Swiss Hepato-Pancreato-Biliary Center, Department of Visceral and Transplantation Surgery, Zurich University Hospital, Zurich 8091, ZH, Switzerland

Giovanni Pellegrini, Institute of Veterinary Pathology, University of Zurich, Zurich 8057, ZH, Switzerland

Corresponding author: Simone Mafalda Rodrigues Camargo, PhD, Pharmacist, Senior Scientist, Institute of Physiology, University of Zurich, Winterthurerstrasse 190, Zurich 8057, ZH, Switzerland. simone.camargo@physiol.uzh.ch

Abstract

BACKGROUND

The expression of amino acid transporters is known to vary during acute pancreatitis (AP) except for LAT1 (*slc7a5*), the expression of which remains stable. LAT1 supports cell growth by importing leucine and thereby stimulates mammalian target of rapamycin (mTOR) activity, a phenomenon often observed in cancer cells. The mechanisms by which LAT1 influences physiological and pathophysiological processes and affects disease progression in the pancreas are not yet known.

AIM

To evaluate the role of LAT1 in the development of and recovery from AP.

METHODS

AP was induced with caerulein (cae) injections in female and male mice expressing LAT1 or after its knockout (LAT1 Cre/LoxP). The development of the initial AP injury and its recovery were followed for seven days after cae injections by daily measuring body weight, assessing microscopical tissue architecture, mRNA and protein expression, protein synthesis, and enzyme activity levels, as well as by testing the recruitment of immune cells by FACS and ELISA.

RESULTS

The initial injury, evaluated by measurements of plasma amylase, lipase, and

trypsin activity, as well as the gene expression of dedifferentiation markers, did not differ between the groups. However, early metabolic adaptations that support regeneration at later stages were blunted in LAT1 knockout mice. Especially in females, we observed less mTOR reactivation and dysfunctional autophagy. The later regeneration phase was clearly delayed in female LAT1 knockout mice, which did not regain normal expression of the pancreas-specific differentiation markers recombining binding protein suppressor of hairless-like protein (rbpjl) and basic helix-loop-helix family member A15 (mist1). Amylase mRNA and protein levels remained lower, and, strikingly, female LAT1 knockout mice presented signs of fibrosis lasting until day seven. In contrast, pancreas morphology had returned to normal in wild-type littermates.

CONCLUSION
LAT1 supports the regeneration of acinar cells after AP. Female mice lacking LAT1 exhibited more pronounced alterations than male mice, indicating a sexual dimorphism of amino acid metabolism.

Key Words: Acute pancreatitis; Amino acid transporter; LAT1; Metabolism; Regeneration; Fibrosis

Core Tip: LAT1 (*slc7a5*) transports amino acids into cells and is an upstream regulator of metabolic signaling pathways. This transporter was shown to play an important role in highly proliferative cells during embryonic development and cancer, controlling protein synthesis and cell proliferation. In this study we provide evidence that LAT1 plays a role in the pancreatic acinar regeneration after acute pancreatitis. Additionally, knocking down LAT1 revealed a sex difference in the regenerative process, which may be supportive to understand gender differences in the clinical setting.

Citation: Hagen CM, Roth E, Graf TR, Verrey F, Graf R, Gupta A, Pellegrini G, Poncet N, Camargo SMR. Loss of LAT1 sex-dependently delays recovery after caerulein-induced acute pancreatitis. *World J Gastroenterol* 2022; 28(10): 1024-1054
URL: https://www.wjgnet.com/1007-9327/full/v28/i10/1024.htm
DOI: https://dx.doi.org/10.3748/wjg.v28.i10.1024

INTRODUCTION

Acute pancreatitis (AP), an inflammatory disease of the exocrine pancreas, ranks among the most frequent gastrointestinal causes for hospital admission in the United States[1]. AP is mainly provoked by gallbladder stones, alcohol overconsumption, or other toxic substances disturbing the tightly regulated function of the exocrine pancreas[2]. The disease most often has a mild course with interstitial inflammation; however, it can also be severe with necrosis and detrimental complications. In severe, prolonged, or repetitive cases, sustained inflammation leads to expansion of extracellular matrix components, altering pancreatic architecture and replacing functional tissue. Significant fibrosis is accompanied by exocrine and endocrine insufficiency. It represents a risk factor for oncogenic transformation, seriously reducing life quality and expectancy[3,4].

Several theories have been suggested over the last decades to explain the pathogenesis of AP. Self-digestion following premature intrapancreatic activation of enzymes has become the most accepted one [5]. The disruption of various systems, leading to calcium signaling impairment, endoplasmic reticulum (ER) stress, and autophagy dysregulation[6], have been shown to lead to intrapancreatic trypsin activation. When activated prematurely upon internal or external influences, the digestive enzymes may provoke acinar cell death by autolysis, thereby triggering AP. This results not only in local but also systemic inflammatory responses. Activation of the immune system is a further crucial player in AP. Acinar cells themselves produce and release cytokines that attract neutrophils and macrophages, which influence the course of the inflammation[7].

Fundamental changes accompany the process of injury and regeneration of the tissue. They lead to an altered morphological appearance, reflecting a shift in the molecular expression profile that ultimately modifies the functional properties of the cells. Besides edema, inflammatory cell invasion, and cell death, reduction of digestive enzymes storage in zymogen granules has been observed. In addition, acinar-to-ductal metaplasia (ADM)[8] occurs, transforming the pancreas' phenotypical layout. Secretory acinar cells transiently dedifferentiate into pancreatic progenitor-like cells with embryonic properties, with a reduction of protein synthesis and a high proliferative capacity. They recover the capacity to

express embryonic transcription factors (*e.g.*, sox9, pdx1) and reduce the expression of markers characteristic of functionally differentiated cells (*e.g.*, PTFA1 complex, mist1/Bhlha15, digestive enzymes)[9]. This exerts a positive effect on the regenerative process, as shown by the fact that preventing ADM aggravates damage in AP[10].

Acinar cells are responsible for the synthesis, storage, and secretion of more than 200 different proteins. In these cells, approximately 70% of the total mRNA encodes for secreted proteins[11]. Translation is controlled by the mammalian target of rapamycin (mTOR) pathway[12] and induced by amino acid uptake[13,14]. Willet *et al*[15] proposed a stepwise adaptation of metabolic phases during AP, starting with an initial downregulation of the exocrine function and the activity of the mTOR pathway, followed by the activation of autophagy and dedifferentiation of acinar cells. The surviving cells would enter a quiescent phase and recycle cellular components to uphold their energy balance instead of producing secretory proteins. Subsequent proliferation and mTOR reactivation combined with the restoration of digestive capacity would reconstitute the healthy state.

Amino acids are actively transported into acinar cells to provide the necessary building blocks for protein synthesis. An influence on amino acid transporters (AAT) by diet[16] and early AP injury[17] has been shown in our previous work. We identified the localization of the glutamine and neutral amino acid transporters LAT1 (*slc7a5*), LAT2 (*slc7a2*), SNAT3 (*slc38a3*), and SNAT5 (*slc38a5*) at the basolateral membrane of acinar cells. In a healthy pancreas, Na^+-dependent SNAT3 and SNAT5 transport amino acids, such as glutamine, with a low affinity and high capacity into the cell[18]. These amino acids accumulate in the cells and serve as exchange substrates to uptake other amino acids such as leucine, transported by the antiporters LAT1 and LAT2[19]. During early injury of AP, SNAT3 and SNAT5 were strongly reduced. At the same time, LAT1 expression was preserved both at the mRNA and protein levels, suggesting that in LAT1 case, AAT may play a role in supporting the survival of remaining acinar cells rather than supporting secretory protein synthesis. Moreover, in a cell culture model mimicking pancreatitis, loss of LAT1 expression was associated with dedifferentiation and expression of senescence genes (*e.g.*, ptf1a, pdx, sox9, p21), further supporting its importance in maintaining acinar cell identity and survival[17,20].

LAT1 (*slc7a5*) and CD98 glycoprotein (*slc3a2*) form a heterodimeric antiporter selective for several essential neutral amino acids that are ubiquitously expressed, particularly in the brain, exocrine glands, testes, and immune cells[21]. Notably, LAT1 is highly active in proliferating cells with physiological importance during immune cell activation[22] or placental development, and its ablation causes early intrauterine death[23]. So far, this transporter has been studied mainly in cancer[24], where its overexpression promotes growth by delivering substrates and influencing various signaling pathways. Particularly, mTOR is activated by leucine transported through LAT1[25]. mTOR prompts survival and proliferation of the cells, explaining the role of LAT1 as a negative prognostic marker in cancers such as pancreatic ductal adenocarcinoma (PDAC)[26]. Moreover, enhanced endothelial LAT1 stimulates angiogenesis and thereby further boosts tumor progression[27].

The maintained presence of LAT1 during initial AP injury might support a pro-proliferative state favoring regeneration. In this study, we analyzed the role of AAT during the recovery of AP, especially focusing on LAT1. The results presented here illustrate the importance of sustained expression of LAT1 during the initial injury phase to ensure complete regeneration.

MATERIALS AND METHODS

Acute pancreatitis in wild-type and LAT1 knockout mice

The experiments were performed in C57Bl/6 (Jackson Laboratories) and LAT1-Cre/LoxP (obtained by crossing the Slc7a5$^{flox/flox}$ strain (B6.129P2-*Slc7a5tm1.1Daca*/J) with the B6.129-Gt(ROSA)26Sor-tm1(cre/ERT2)Tyj/J)[28,29] mice, as approved by the Zurich Cantonal Veterinary office (License ZH075/15) and handled in accordance with the Swiss Animal Welfare law and good laboratory practice. Mice were group-housed in standard conditions of controlled temperature (21-24 °C) and 12 h light-dark cycles and fed standard chow (#3436 Kliba Nafag, Kaiseraugst, Switzerland) and drinking water ad libitum.

At 2-3 mo of age, AP was induced *in vivo* by administering the secretagogue caerulein (cae) (Sigma, Louis, MO, United States) in twelve intraperitoneal injections of 50 μg/kg body weight at hourly intervals. LAT1 knockout was induced by tamoxifen (Sigma-Aldrich, Buchs, Switzerland) oral gavage 160 mg/kg for three consecutive days. LAT1 cre- wild-type (LAT1-wt) and LAT1 cre+ knockout (LAT1-ko) mice were treated with tamoxifen to rule out the possible effects of tamoxifen alone. AP in LAT1-wt and LAT1-ko mice was induced seven days after the first tamoxifen gavage, as control served animals injected with saline in the same regimen. Following treatment, blood samples were withdrawn for plasma analysis at the end of cae injections (12 h) with heparin coated capillary tubes from the tail, and body weight was measured daily until animals were sacrificed at specific time points between 24 h up to seven days after the first injection of cae or saline.

The sacrifice procedure was performed under inhalation anesthesia with isoflurane (Attane, Piramal Critical Care, Inc., Bethlehem, PA, United States). Tissue from the pancreas tail was obtained for RNA extraction immediately after laparotomy, snap-frozen in liquid nitrogen, and stored at -80 °C to avoid autodigestion. After heart blood drawing, a high dose of isoflurane was applied until all vital signs were terminated. The remaining pancreas was collected, snap-frozen in liquid nitrogen for protein analysis, or fixed in 3% paraformaldehyde (PFA) for 24 h and embedded in paraffin for subsequent microscopical analysis using the Microtom STP 120 (MICROTOM International, Walldorf, Germany) by immersion in progressive gradients of ethanol, Xylol, and paraffin, applying a standard protocol.

Measurement of plasma amylase and lipase

Twelve or 24 h after the first injection of cae or saline, plasma was collected by centrifugation (5 min at 8000 x g and 4 °C) of heparinized blood samples and kept at -80 °C until measurements were made. Measurement was done according to the manufacturer's instructions (Fuji Dri-Chem 4000i).

Hematoxylin/eosin and Masson's trichrome staining

The samples for the initial morphological analysis of wild-type mice (C57Bl/6) were collected from 24 h to seven days after the first injection of cae or saline. For LAT1 cre-inducible mice (LAT1-Cre/LoxP), samples were collected three and seven days after the first injection of cae or saline. The paraffin-embedded pancreas was sectioned (5 µm) and stained with hematoxylin/eosin (HE) or Masson's trichrome using a standard protocol. The morphological analysis for HE was performed on the scanned slides (Nanozoomer HT 2.O, Hamamatsu, Japan) from the Laboratory for Animal Model Pathology (LAMP) at the University of Zurich. A 40 x magnification was used (objective lens magnification of x 40, eyepiece magnification of x 10), and the analysis to grade the different stages of AP was done in a blinded fashion. Tissue injury was morphometrically graded according to edema, inflammatory cell invasion, and ADM using the slide viewer NDP.view 2 (HAMAMATSU PHOTONICS K.K., Japan). Edema was scored from 0 to 3 (0 for no edema present, 3 for most pronounced edema) depending on subjective interlobular space. The presence of inflammatory cells was quantified in ten randomly chosen microscopic fields of 0.1 mm^2 in 40 x magnification. ADM was quantified as percentage of metaplasia in relation to total exocrine pancreatic tissue. The morphological analysis of Masson's trichrome staining was done using a Nikon Eclipse TE300 epifluorescence microscope (Nikon Instruments Inc., Melville, NY) equipped with a DS-5 M Standard charge-coupled device camera (Nikon Instruments Inc.). The score was performed blind by two independent observers.

Immunohistochemistry and immunofluorescence

Immunohistochemistry was performed on 5 µm paraffin-embedded tissue slides using the Dako Autostainer Universal Staining System Model# LV-1 and the Leica BOND RX according to the supplier's instructions. The analysis was performed on the scanned slides using the slide viewer NDP.view 2. Stained acinar cells were quantified in ten randomly chosen microscopic fields of 0.1 mm^2 in 40 x magnification. For immunofluorescence, the slides were deparaffinized in a Microm spin tissue processor STP-120, reversing the steps of immersion. Antigen retrieval was performed in the pressure cook (HistosPRO (SW 2.0.0), Rapid Microwave Histoprocessor) as described in Table 1. After antigen retrieval, sections were blocked (2% BSA, 0.04% Triton X-100 in PBS, pH 7.4) and incubated with the primary antibody. The appropriate secondary antibodies were added, and nuclei were stained with 4′,6-diamidino-2-phenylindole (Dapi, Thermo Fischer Scientific, Waltham, MA, United States). Sections were mounted using a Dako Glycergel mounting medium (DakoCytomation, Glostrup, Denmark).

The sections were analyzed with a Nikon Eclipse TE300 epifluorescence microscope (Nikon Instruments Inc., Melville, NY) equipped with a DS-5 M Standard charge-coupled device camera (Nikon Instruments Inc.). Pictures were acquired with NIS Elements (Nikon Instruments Inc.) and processed in Photoshop 9.

Western blotting

The samples for protein analysis by Western blotting were collected 24 h and three days after the first injection of cae or saline. Pancreas samples were fractioned into membrane and cytosol components for AAT analysis as previously described[17]. Briefly, tissue was homogenized in an ice-cold resuspension buffer (200 mmol/L mannitol, 80 mmol/L HEPES, 41 mmol/L KOH, protease inhibitor, pH 7.5) using beads (MagNALyser Green Beads, Roche, Switzerland) for 2 × 30 s 6000 rpm in a tissue homogenizer (Precellys® 24, Bertin Technologies, France). After an initial centrifugation step (15 min at 800 × g, 4 °C), cytosol and membrane were obtained by ultracentrifugation (1 h at 100000 × g, 4 °C). To prepare a total lysate, tissue was homogenized in an ice-cold RIPA buffer (20 mmol/L Tris-HCl pH 7.5, 150 mmol/L NaCl, 1 mmol/L Na_2EDTA, 1 mmol/L EGTA, 1% NP-40, 1% sodium deoxycholate, 2.5 mmol/L sodium pyrophosphate, 1 mmol/L β-glycerophosphate, 1 mmol/L Na_3VO_4, 1 µg/mL leupeptin, protease inhibitor, pH 7.5). The tissue was homogenized (2 × 20 s 5500 rpm) and sonicated, and samples were centrifuged (20 min at 16000 × g, 4 °C). The supernatant representing total lysate was used to analyze amylase, eukaryotic translation initiation factor 2α (eIF2α), microtubule-associated proteins 1A/1B light chain 3B (LC3), ubiquin-binding protein p62, S6 kinase (S6K), smooth muscle actin (SMA), and

Table 1 Antibodies and conditions applied in immunohistochemistry and immunofluorescence experiments

Antigen	Antigen retrieval	Primary antibody	Antibody dilution
Amylase	SDS 0.1%	LifeSpan BioSciences, Inc. (LS-B8239)	1:1000
Caspase 3	Sodium citrate pH 6	Cell Signaling (9664)	1:400
E-cadherin	Tris-EDTA pH 9	Invitrogen (13-1900)	1:200
LAT1	Tris-EDTA pH 9	Cosmo Bio (KE026)	1:100
pH3	Sodium citrate pH 6	Merk-Sigma (06-570)	1:1000
SMA	Sodium citrate pH 6	Abcam (AB5694)	1:500
SNAT5	Tris-EDTA pH 9	Pineda (599341)	1:2000

pH3: Phosphohistone 3; SMA: Smooth muscle actin.

vimentin. Protein content was measured by a modified Lowry method (Biorad, Hercules, CA) according to the manufacturer's instructions. Samples were separated on sodium dodecyl sulfate polyacrylamide gels (SDS-PAGE) and transferred electrophoretically to a polyvinylidene difluoride (PVDF) membrane (Immobilon-P, Millipore, Bedford, MA, United States). The membranes were blocked and incubated with antibodies, as described in Table 2.

Protein was identified by a chemiluminescent method (Merck Millipore, Darmstadt, Germany) and detected with the luminescent image analyzer FujiFilm LAS-4000 camera (GE Healthcare, Glattbrugg, Switzerland) according to the manufacturer's instructions. Densitometric quantification of the bands was performed using the software ImageJ (National Institutes of Health, Bethesda, MD, United States).

RNA extraction and qPCR

The samples for RNA extraction were collected 24 h, three days, and seven days after the first injection of cae or saline. Total RNA was extracted using RNeasy Mini Kit (Qiagen, Basel, Switzerland), and tissue was homogenized using beads (Precellys® 24, Bertin Technologies, France). The RNA quality control was performed by microchip analysis Agilent 2100 Bioanalyzer (NanoChip, Agilent Technologies, Santa Clara, CA, United States) with a minimal required RIN of 7.0. Reverse transcription was performed according to the manufacturer's instructions, and 10 ng cDNA was added to Taq-Man Universal PCR master mix (Applied Biosystems) using a Prism 7700 cycler (Applied Biosystems, Foster City, CA, United States). The primers and probes used in this study not yet published[16,17,30,31] are listed in Table 3.

The mRNA expression of the gene of interest (GOI) relative to that of the housekeeping gene (HKG, 18S) was calculated by applying the Delta CT method ($r = 2^{[Ct(HKG)-Ct(GOI)]}$).

Assays for trypsin activated, MPO, and MCP1

The samples collected 24 h after the first injection of cae or saline were prepared according to Lau and Bhatia [32]. Briefly, one-fourth of the pancreas was homogenized with MagNALyser Green Beads (Roche, Switzerland) and ice-cold 10 mmol/L sodium phosphate buffer pH 7.4 using a Precellys® 24 tissue homogenizer (Bertin Technologies, France) for 2 × 30 s 6800 rpm. DNA was determined in the total lysate, and the supernatant was used for trypsin, myeloperoxidase (MPO), and monocyte chemotactic protein 1 (MCP1) measurements. As previously described[33], trypsin activity was measured using Boc-Q-A-R-MCA (BACHEM, Bubendorf, Switzerland) as substrate. The activity of trypsin was normalized to DNA and expressed as nmol/μg DNA. MPO measurement was determined with 3,3′,5,5′-Tetramethylbenzidine (TMB, Sigma) after 2 minutes incubation. The final MPO activity was normalized to DNA and expressed as fold change to control samples. MCP1 was measured by ELISA (R&D Systems, Inc., Minneapolis, MN, United States) according to the manufacturer's instructions, and the final concentration of MCP1 was expressed as pg/μg DNA. DNA was quantified using a fluorescence Quantitation Kit (Sigma-Aldrich, St. Louis, MO) according to the manufacturer's instructions.

FACS

The pancreas of mice 24 h after the first injection of cae were excised and immediately digested with collagenase (1 mg/mL) and DNAaseI (100 U/mL) and filtered through a 40 μm filter to remove debris. The single-cell suspension was incubated for 30 min at 4 °C with a master mix of antibodies targeting cell surface markers for lymphocytes (CD8a, NK1.1, CD4, CD45.2) or myeloid cells (CD11b, Ly6G, Ly6C, CD62L, CD45.2). After washing and fixing with 2% PFA, samples were acquired using FACS Canto II (BD Biosciences). Flow cytometry data were analyzed using FlowJo v10.7.1 software (Tree Star Inc.).

Table 2 Antibodies and conditions applied in Western blotting experiments

Antigen	Total protein loaded (μg)	Primary antibody	Antibody dilution
Amylase	2.5	LifeSpan BioSciences, Inc. (LS-B8239)	1:10000
β-tubulin	Varying	Sigma (T8328)	1:5000
LAT1	20	Cosmobio (KE026)	1:500
LC3	100	MLB (PM036)	1:250
NA/K-ATPase	Varying	Santa Cruz (sc-48345)	1:10000
p62	50	MBL (PM045)	1:1000
peIF2α	25	Cell Signaling (3398)	1:1000
pS6K	50	Cell Signaling (9205S)	1:1000
SMA	25	Sigma (C6198)	1:1000
teIF2α	25	Cell Signaling (9722)	1:1000
tS6K	50	Cell Signaling (2708P)	1:1000
Vimentin	30	Invitrogen (MA5-11883)	1:1000

LC3: Microtubule-associated proteins 1A/1B light chain 3B; peIF2: Phosphorylated eukaryotic translation initiation factor 2; pS6K: Phosphorylated S6 kinase; SMA: Smooth muscle actin; teIF2α: Total eukaryotic translation initiation factor 2α; tS6K: Total S6 kinase.

Incorporation of leucine in protein to determine protein synthesis

Protein synthesis was analyzed 24 h and three days after the first injection of cae or saline. Food was removed at least one hour before mice received gavage containing 1.5 mmol/L leucine and H^3-leucine (0.7 μCi/10 g of body weight). Mice were anesthetized, and 15 min after the gavage, the blood and pancreas were collected. The organ was cut into four pieces, weighed, and snap-frozen. Serum was used to calculate the specific radioactivity by measuring total leucine by ultra performance liquid chromatography[16] and the radioactive leucine. The tissue was homogenized in 0.6 M perchloric acid using beads and a Precellys system (2 × 30 s 6800 rpm) and incubated for one hour on ice. The pellet was obtained by centrifugation (15 min at 10000 × g), washed, and resuspended in 0.3 M sodium hydroxide. The resuspended pellet was used for the measurement of total protein and incorporated radiolabeled leucine. The rate of protein synthesis was expressed as pmol of leucine incorporated into protein per hour (pmol leu /mg protein/hour) as previously described[12].

Statistics

Data were analyzed and represented in GraphPad Prism 5 (GraphPad Software, San Diego, CA, United States) as means ± standard error of the mean (SEM). Statistical comparison between LAT1-wt and LAT1-ko groups at various time points of pancreatitis was done by unpaired two-tailed student's *t*-test or one-way ANOVA with Bonferroni post hoc test. *P* values of 0.05 or less were regarded as statistically significant and labeled as $^aP \leq 0.05$, $^bP \leq 0.01$, $^cP \leq 0.001$.

RESULTS

LAT1 amino acid transporter expression differs from other transporters during AP injury and regeneration

Expression of AAT was analyzed in a model for AP and correlated with morphology, dedifferentiation, and functional markers. AP initial injury was histologically evidenced by the invasion of inflammatory cells and interstitial edema (Figure 1A), peaking one to two days after AP induction (Figure 1B and C). On days three and four after the first injection of cae, the most dedifferentiated structures appearing as ADM were observed throughout the tissue (Figure 1D). Besides the formation of ADM crucial for regeneration[34], dedifferentiation and reduction of specific organ function were also characterized by the expression of known indicator genes. As depicted in Figure 1E, cytokeratin 19 (ck19) expression as a very early marker for dedifferentiation rose and was sustained throughout the period during which ADM was observed. Pancraes associated transcription factor 1a (ptf1a), which with recombining binding protein suppressor of hairless-like protein (rbpjl) forms the pancreas transcription factor 1 (PTF1) complex determining pancreatic fate and supporting acinar cell function[35], transiently increased two-fold. Additionally, an increased expression of SRY-box transcription factor 9 (sox9) coincided with the presence of ADM structures, as previously noted[36,37]. On days three and four,

Table 3 Primers and probes for mouse genes used in qPCR

Gene	Primers	Probe (Universal Probe Library Roche)	Accession No.
Amylase 2A4			
S	TGATGACTGGGCTTTGTCAG	4	NM_001160150.1
AS	GCCATCGACCTTATCTCCAG		
ccnb2			
S	CAACCGTACCAAGTTCATCG	3	NM_007630.2
AS	GATGGCAGTCCAGTGTCTAGG		
CD206			
S	CCTTGAACCCATTTATCATTCC	49	NM_008625.2
AS	CTGTAGCAGTGGCCTGCAT		
ck19			
S	AGTCCCAGCTCAGCATGAA	97	NM_008471.3
AS	TAACGGGCCTCCGTCTCT		
Clusterin			
S	AAGTACTACCTTCGGGTCTCCA	6	NM_013492.3
AS	AGCTTCACCACCACCTCAGT		
col4a1			
S	GGCCCTTCATTAGCAGGTG	9	NM_009931.2
AS	TCTGAATGGTCTGACTGTGTACC		
cpa1			
S	CCCCTATGGCTACACATCAGA	63	NM_025350.4
AS	TCCCGTGTAGAGATGTCAAGG		
ctsb			
S	AAGCTGTGTGGCACTGTCCT	72	NM_007798.3
AS	GATCTATGTCCTCACCGAACG		
ctsd			
S	CCCTCCATTCATTGCAAGATAC	3	NM_009983.2
AS	TGCTGGACTTGTCACTGTTGT		
ctsl			
S	ACAGAAGACTGTATGGCACGAA	25	NM_009984.4
AS	GGATCATTCTCATGTTCTTCTCC		
Elastase			
S	ACGGAGCACCCTGTTACATC	22	NM_026419.2
AS	CTGCTGCAGCTTGTCTGG		
F4/80			
S	AGGAGGACTTCTCCAAGCCTA	67	NM_010130.4
AS	AGGCCTCTCAGACTTCTGCTT		
icam-1			
S	GCTACCATCACCGTGTATTCG	53	NM_010493.3
AS	AGGTCCTTGCCTACTTGCTG		
IL-1β			

S	AGTTGACGGACCCCAAAAG	38	NM_008361.4
AS	AGCTGGATGCTCTCATCAGG		
IL-6			
S	GCTACCAAACTGGATATAATCAGGA	6	NM_031168
AS	CCAGGTAGCTATGGTACTCCCGAA		
IL-10			
S	CAGAGCCACATGCTCCTAGA	41	NM_010548.2
AS	TGTCCAGCTGGTCCTTTGTT		
lipase			
S	GCCACGATGCTAATGCTGT	3	NM_026925.3
AS	ATCACTGAAGCAGCCGAGTT		
mist1			
S	GGCTAAAGCTACGTGTCCTTG	77	NM_010800.3
AS	GCTCCAGGCTGGTTTTCC		
nox2			
S	TGCCAACTTCCTCAGCTACA	20	NM_007807.5
AS	GTGCACAGCAAAGTGATTGG		
p21			
S	TTGCCAGCAGAATAAAAGGTG	9	NM_001111099.2
AS	TTTGCTCCTGTGCGGAAC		
p27			
S	GTTAGCGGAGCAGTGTCCA	62	NM_009875.4
AS	TCTGTTCTGTTGGCCCTTTT		
p62			
S	AACTGGAGCCCACGTCCT	22	NM_001290769.1
AS	CTCCCCCACATTCTTCAGG		
prss1+3			
S	CTGCTGGCACTCAGTGTCTC	20	NM_053243.2
AS	GCAGGTCTGGTTCACTGACA		
prss2			
S	CCAGAGTGGCCTCTGTACCT	20	NM_009430.2
AS	AGCAGGTCTGGGTTGTTCAC		
ptf1a			
S	GCTTGGCCATAGGCTACATT	73	NM_018809.2
AS	GGACTGTCCTCTCCGAGGT		
rbpjl			
S	TCAGAAATCCTATGGAAATGAGAA	20	NM_009036.1
AS	GGTCTTGCATTGGCTTCAC		
sma/Acta2			
S	TAACCCTTCAGCGTTCAGC	20	NM_007392.3
AS	ACATAGCTGGAGCAGCGTCT		
sox9			
S	CAGCAAGACTCTGGGCAAG	25	NM_011448.4

AS	ATCGGGGTGGTCTTTCTTGT		
spink1			
S	CACCCAGATCTTCGACAATG	83	NM_009258.5
AS	TAAACTCAGCAGGGCCAAAG		
tnfα			
S	CTGTAGCCCACGTCGTAGC	25	ENSMUST00000025263
AS	TTTGAGATCCATGCCGTTG		
tgfβ			
S	CTCAGAGCAAGAGAAAGCACTG	3	NM_001164074.1
AS	CGTTGATGAACCAGTTACAGACC		
Vimentin			
S	CGAGGAGAGCAGGATTTCTC	53	NM_011701.4
AS	GGAAGTGACTCCAGGTTAGTTTCTC		

ccnb2: Cyclin b2; CD206/Mrc1: macrophage mannose receptor C type 1,ck19: Cytokeratin 19; col4a1: Collagen type IV alpha 1 chain; cpa1: Carpoxypeptidase 1; ctsb: Cathepsin b; ctsd: Cathepsin d; ctsl: Cathepsin l; icam-1: Intercellular adhesion molecule 1; IL-1: Interleukin 1; IL-6 and 10: Interleukin 6 and 10; mist1: Basic helix-loop-helix family member A15; nox2: NADPH oxidase 2; p21/cip/Cdkn1a: Cyclin Dependent Kinase Inhibitor 1A; p27/kip/Cdkn1b: cyclin-dependent kinase inhibitor 1B, prss1+3: Serine protease 1+3; prss2: Serine protease 2; ptf1a: Pancreas associated transcription factor 1a; rbpjl: Recombining binding protein suppressor of hairless-like protein; sma/Acta2: α smooth muscle actin/alpha-actin-2; sox9: SRY-box transcription factor 9; spink1: Serine peptidase inhibitor kazal type 1; tnfα: Tumor necrosis factor α; tgfβ: Transforming growth factor β.

when dedifferentiation was highest, we observed a peak expression of the M-phase mitosis indicator, cyclin b2. In contrast, the expression of differentiation and functional acinar cell genes, rbpjl and basic helix-loop-helix family member A15 (mist1), declined quickly in the initial injury phase along with mRNA levels of amylase and carboxypeptidase 1 (cpa1) (Figure 1F). Diverging from rbpjl and mist1, mRNA levels of amylase and cpa1 lagged at still lower to normal levels after seven days, indicating incomplete functional recovery despite the near-normal morphological appearance of the tissue. The decrease of enzyme expression as functional acinar cell markers and a decrease in protein synthesis would be expected to correlate with the decreased expression of AAT. Such a parallel regulation could indeed be nicely observed with the expression of the sodium-dependent transporter for neutral amino acids SNAT5 (*slc38a5*) and, to some extent, for SNAT3 (*slc38a3*) (Figure 1G). The expression of SNAT5, however, did not return to normal levels during seven days, similar to amylase and cpa1. On the other hand, the mRNA expression of the amino acid exchangers for neutral amino acids LAT1 (*slc7a5*) and LAT2 (*slc7a8*) was increased (Figure 1H). It should be noted that, at the protein level, LAT1 decreased (Figure 1I) but persisted along the course of the disease. Immunofluorescence showed that LAT1 was still expressed in the remaining acinar (Figure 1J) and ADM cells alike. During regeneration (three days after AP induction), LAT1 was localized in ADM, where the expression of the epithelial cell marker E-cadherin was lost (Figure 1K). This suggests that LAT1 impacts survival and recovery of acinar cells during AP, maintaining a relatively steady expression, in contrast to SNAT5 that declined after AP induction (Figure 1J).

A pancreas lacking LAT1 expression showed similar acute pancreatitis-induced early injury to a wild-type pancreas

A LAT1 inducible whole-body knockout (LAT1 cre- wild-type "LAT1-wt" and LAT1 cre+ knockout "LAT1-ko") model was used to analyze whether LAT1 plays a role in the regeneration of the pancreas during AP, and the timeline of the experiments is depicted in Figure 2A. The knockout of LAT1 induced with tamoxifen was demonstrated to be efficient at the mRNA level and was maintained throughout the experimental observation (Figure 2B). Moreover, the mRNA results corresponded with the disappearance of protein in the tissue (Figure 2C and D). The ablation of LAT1 did not induce a compensatory overexpression of other AAT, and the levels of LAT2, xCT, SNAT2, SNAT3, and SNAT5 did not differ between genotypes or sexes (Figure 2E).

The severity of AP was analyzed by plasma amylase and lipase levels, neutrophils' and macrophages' recruitment and activity and trypsin activation. Pathways of metabolic adaptation and autophagy capacity were examined together with AAT expression and protein synthesis of the exocrine pancreas.

After inducing AP in LAT1-wt and LAT1-ko mice, the levels of plasma amylase and lipase measured 12 h after the first cae injection were elevated, confirming the development of AP (Figure 2F). Additionally, we observed a sex difference concerning the enzyme levels. Amylase ($P < 0.05$ for LAT1-ko) and lipase ($P < 0.01$ for LAT1-wt) were higher in male than in female mice 12 h after the first cae

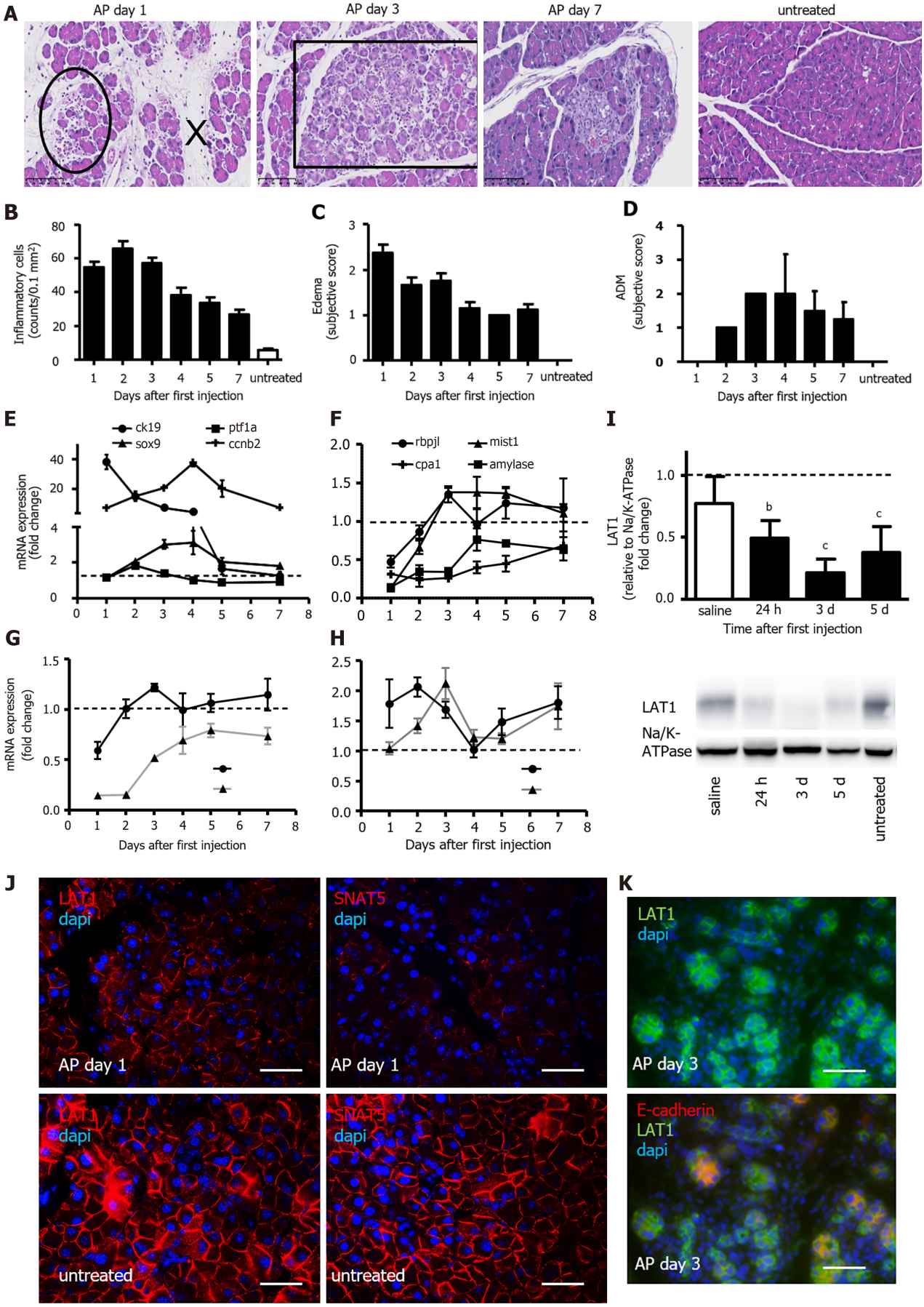

Figure 1 During recovery from acute pancreatitis, the expression of the amino acid transporter LAT1 was changed in a different way alongside dedifferentiation and the appearance of maturity markers for acinar cells. A-D: Morphological analysis of the pancreas after the induction

of acute pancreatitis (AP). A: HE stain depicting changes during the observed time period. Circle: inflammatory cells, x: edema, square: acinar-to-ductal metaplasia (ADM); B: Quantification of inflammatory cells as counts per 0.1 mm^2 field; C: Edema; D: ADM score from 0 to 3; E-F: Variation of dedifferentiation and maturity markers over seven days; mRNA expression for genes of E: dedifferentiation (ck19, SRY-box transcription factor 9 (sox9), pancreas associated transcription factor 1a (ptf1a)) and proliferation (cyclin b2 (ccnb2)) as well as F: organ-specific maturity (recombining binding protein suppressor of hairless-like protein (rbpjl), basic helix-loop-helix family member A15 (mist1), amylase, and carboxypeptidase 1 (cpa1)) in pancreas was analyzed *via* qPCR and expressed as a fold change that was compared to untreated controls, $n = 4$. The line indicates the expression level found in the control animals; G-H: Variations of amino acid transporter (AAT) gene expression alongside injury and regeneration. mRNA expression of G: SNAT3 (*slc38a3*) and SNAT5 (*slc38a5*) and H: LAT1 (*slc7a5*) and LAT2 (*slc7a8*) was examined *via* qPCR and expressed as a fold change that was compared to untreated controls ($n = 4$). The line indicates the expression level found in the control animals; I-K: LAT1 expression decreased but did not disappear during injury and regeneration; I: LAT1 protein was analyzed with Western blotting (10% SDS-PAGE gel and membrane fraction of cell lysates), and it showed a band at approximately 39 kDa. The results were expressed relative to Na/K-ATPase and were normalized in line with untreated animals. The line represents the level in untreated animals. Mean ± SEM, $n = 4$. Statistical analysis was conducted with ANOVA and Bonferroni and then compared with the saline-injected negative control. $aP < 0.05$, $bP < 0.01$, $cP < 0.001$; J: LAT1 and SNAT5 were located at the basolateral membrane of acinar cells. The paraffin-embedded mouse pancreas was stained red for LAT1 or SNAT5, and the nuclei were stained in blue (4',6-diamidino-2-phenylindole or DAPI). The panels on the left depict LAT1 24 h after AP induction (upper), and the untreated controls are below them. The panels on the right depict SNAT5 24 h after AP (upper) and the untreated controls are shown underneath. The bar length corresponds to 50 μm. K: LAT1 was present in dedifferentiated acinar cells, which were characterized by the absence of E-cadherin co-expression. The paraffin-embedded mouse pancreas was stained for LAT1 (green) and E-cadherin (red), and the nuclei were stained in blue (dapi). The top panel only depicts LAT1, while the bottom panel is overlayed with E-cadherin; in both instances, this is three days after AP induction. The bar length corresponds to 50 μm.

injection. As we showed for wild-type mice in Figure 1, LAT1-wt and LAT1-ko mice from both sexes presented elevated ck19 expression. However, LAT1-ko mice showed more pronounced expression of ck19 than their LAT1-wt littermates, and levels in male mice rose more pronouncedly than in female mice. This indicates a more dedifferentiated state in males, as ck19 is a prominent marker of ADM. The expression of clusterin, another known early injury marker in AP, was also upregulated but did not differ between genotypes or sexes (Figure 2G). Expression of the enzymes amylase, elastase, cpa1, and lipase in the pancreas of control mice (treated with saline) or with AP (24 h after the first cae injection) did not differ between the groups (Figure 2H). This suggests that male and female LAT1-wt and LAT1-ko mice started with the same mRNA levels of these genes, with no sex or genotype differences.

A very early change observed during AP injury is the activation of trypsinogen to trypsin in the pancreas[38]. The activation of trypsin increased after AP induction in both genotypes. Despite the tendency of higher values in LAT1-ko mice, they were spread over a wider range and did not reach significance (Figure 3A). Earlier timepoint measurements (six hours after the first cae or saline injection) confirmed the higher variability in trypsin activation for LAT1-ko mice. They did not statistically differ from LAT1-wt mice (data not shown). The expression at the mRNA level of trypsinogens serine protease 1+3, serine protease 2 (prss1+3, prss2), and trypsin inhibitor serine peptidase inhibitor kazal type 1 (spink1) (Figure 3B) or cathepsins B, D, and L (ctsb, ctsd, and ctsl) (Figure 3C) showed no significant differences in saline-injected control mice for both genotypes and sexes. The transcription of cationic (prss1) and meso (prss3) trypsinogen increased during AP (Figure 3B), differing from other digestive enzymes that decreased (Figure 2H). The basal expression of prss1 and prss3 in LAT1-ko mice was more variable and tended to be higher than in LAT1-wt mice, concomitant with trypsin activity tending to be higher in LAT1-ko mice. The expression of the trypsin inhibitor spink1 remained stable during AP and was only discretely elevated in female LAT1-ko mice with AP (Figure 3B). In cae injected mice, the expression of all cathepsins increased compared to control mice, and mRNA of cathepsins B and D, which modify trypsin activation[39-41], tended to be more abundant in males than females (Figure 3C). These findings do not support a more severe injury but suggest LAT1 ablation interfered with differentiation and caused variable trypsin activation.

The pancreas of mice lacking LAT1 expression showed lower neutrophil recruitment in response to acute pancreatitis

We further analyzed whether LAT1-ko mice developed the same inflammatory reaction regarding neutrophils and macrophages recruitment. Twenty-four hours after AP induction, mRNA for intercellular adhesion molecule 1 (icam-1), which mediates endothelial transmigration of leukocytes, was higher in male LAT1-ko than in female and wild-type mice. The pro-inflammatory cytokine tumor necrosis factor α (tnfα) was found to be lower in female LAT1-ko mice than LAT1-wt mice (Figure 4A). The expression of NADPH oxidase 2 (nox2), an enzyme in phagocytes that produces superoxide, was significantly reduced in LAT1-ko mice (Figure 4A). Myeloperoxidase (MPO) activity (Figure 4B) was also slightly reduced in LAT1-ko mice, implying low neutrophil recruitment. This finding was confirmed by FACS analysis, as Ly6G+ neutrophils were found to be significantly reduced in the LAT1-ko pancreas (Figure 4C). Besides neutrophil recruitment, we analyzed the release of monocyte chemotactic protein 1 (MCP1) by acinar cells and the expression of macrophage marker F4/80. The chemoattractant for macrophages MCP1 was equally increased between genotypes and sexes after AP induction, suggesting similar recruitment of macrophages (Figure 4D). The expression of F4/80 mRNA was elevated during AP and did not differ between genotypes; however, LAT1-ko males showed higher F4/80 mRNA levels than females (Figure 4E). Additionally, the inflammatory cytokines released by

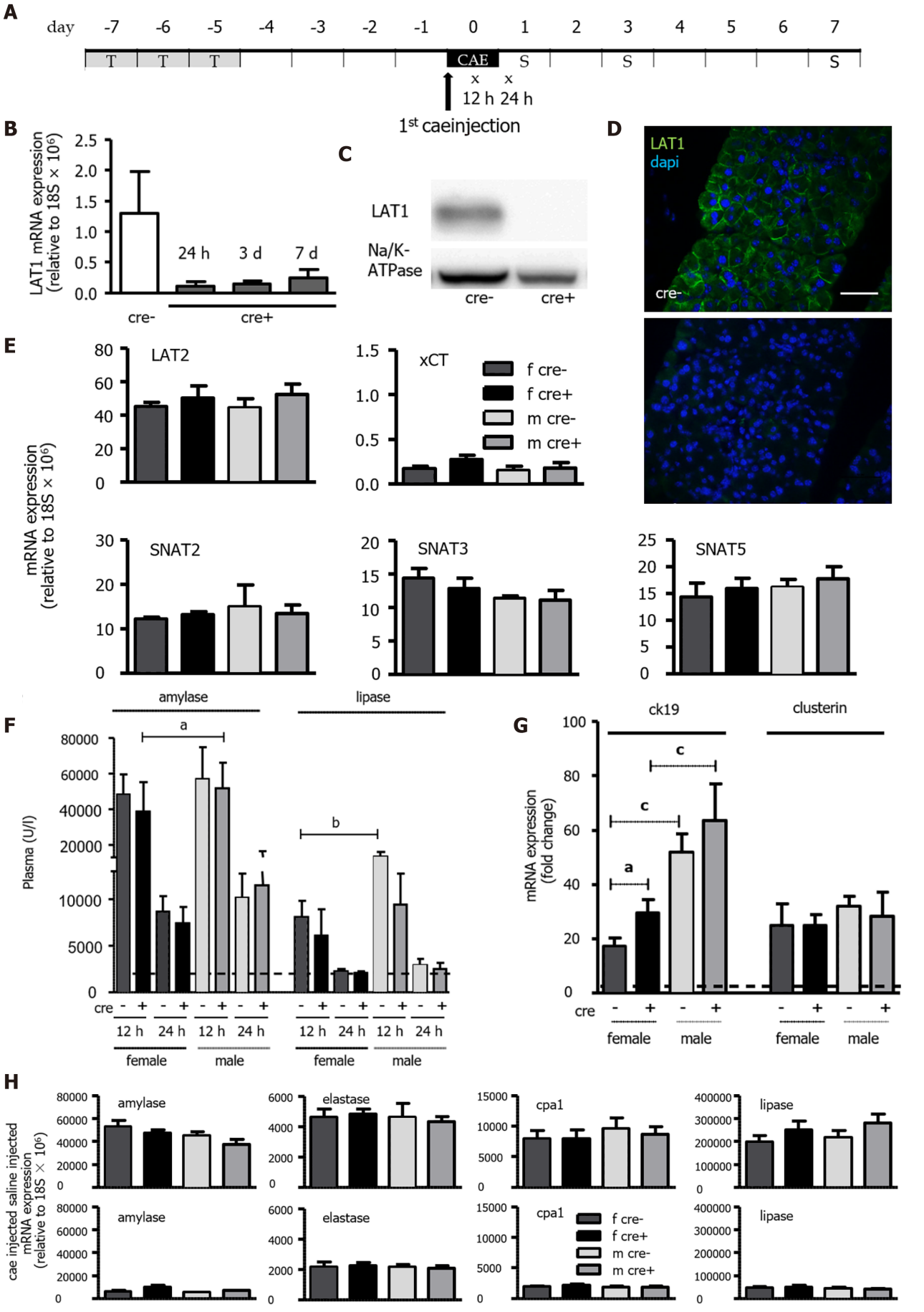

Figure 2 Tamoxifen-induced knockout of LAT1 was efficient in the pancreas, and the mice developed acute pancreatitis in an equivocal

manner. A: Experimental timeline. Three consecutive days of Tamoxifen gavage began seven days prior to acute pancreatitis (AP) induction by caerulein (cae). The first injection of cae marks day zero. Blood for amylase and lipase analysis was drawn 12 and 24 h afterwards (indicated with x). The mice were sacrificed on days one, three, and seven following the first cae injection (indicated with S); B-D: The knockout of LAT1 (*slc7a5*) at the mRNA and protein level was efficient during the period the experiments were conducted. B: mRNA expression for LAT1 was analyzed *via* qPCR and relative to a housekeeping gene (18S × 10^6) in LAT1-ko mice one, three and seven days after the onset of AP, and it was compared to the LAT1-wt mice. C: The LAT1 protein was analyzed with Western blotting (10% SDS-PAGE gel, membrane fraction of cell lysates) three days after the onset of AP, and it displayed a band at approximately 39 kDa. The results were expressed in a manner relative to Na/K-ATPase, and they were normalized in line with untreated animals; D: The paraffin-embedded mouse pancreas was stained for LAT1 (green), and the nuclei were stained in blue (dapi). The top panel depicts LAT1 in LAT1-wt mice, and the bottom is in relation to LAT1-ko mice. The bar length corresponds to 50 μm. E: Neither the knocking out of LAT1 nor the administration of tamoxifen treatment modified the expression of other amino acid transporters (AAT). The mRNA expression of LAT2 (*slc7a8*), xCT (*slc7a11*), SNAT2 (*slc38a2*), SNAT3 (*slc38a3*), and SNAT5 (*slc38a5*) was analyzed *via* qPCR relative to a housekeeping gene (18S × 10^6) in LAT1-wt and LAT1-ko mice treated with tamoxifen and saline. Mean ± SEM, n = 3-8; F: Plasma amylase and lipase increased in LAT1-wt and LAT1-ko mice after the onset of AP. The line indicates the plasma value when it is at a healthy level. Mean ± SEM, n = 7-25; G: LAT1-ko mice exhibited an enhanced presence of dedifferentiation markers. The mRNA expression of cytokeratin 19 (ck19) and clusterin was analyzed *via* qPCR and expressed as a fold change relative to saline-injected controls 24 h after the onset of AP. The line indicates the expression level of the control animals. Mean ± SEM, n = 5-7. H: mRNA expression of amylase, elastase, carboxypeptidase 1 (cpa1), and lipase was analyzed *via* qPCR relative to a housekeeping gene (18S × 10^6), and it was not modified by LAT1 knockout or tamoxifen treatment, yet it decreased after the onset of AP. The upper panel depicts the mice injected with saline, and the lower panel highlights the mice 24 h after AP induction. Mean ± SEM, n = 3-8. The statistical analysis was conducted by ANOVA and Bonferroni, and then it was compared, as indicated by the capped line. $^aP < 0.05$, $^bP < 0.01$, $^cP < 0.001$.

macrophages, interleukin 1β (IL-1β) and interleukin 6 (IL-6), were less expressed in female mice, suggesting a slightly less efficient macrophage recruitment in the female LAT1-ko pancreas following AP induction.

Altogether, our results suggest that despite recruiting less activated neutrophils and macrophages, LAT1-ko mice sustained the same initial injury based on plasma lipase, amylase, and trypsin activation levels.

LAT1 ablation hindered the activation of early regenerative metabolic adaptation

Another characteristic of AP is the fast reduction of function upon injury, with transcription and translation of proteins notably dropping[42,43]. As depicted in Figure 5A, there was a marked reduction in total protein synthesis in mice treated with cae but without difference between genotypes and sexes. Reduction in protein synthesis, inhibition of the mammalian target of rapamycin (mTOR) pathway, autophagy activation, and reactivation of mTOR are important events during the earlier metabolic adaptations and regeneration from AP[15]. As LAT1 is an upstream regulator in the mTOR pathway[25,44], the phosphorylation of its downstream target S6 kinase (S6K) was analyzed. S6K phosphorylation was found significantly reduced in female LAT1-ko mice ($P < 0.05$) during AP (Figure 5B). The phosphorylation of the general control nonderepressible 2 (GCN2) pathway marker eukaryotic translation initiation factor 2α (eIF2α), sensing intracellular shortage of amino acids, was increased in both genotypes during AP (Figure 5C). It was significantly higher in female LAT1-wt mice compared to their male littermates ($P < 0.05$), putatively suggesting accentuated sex-specific nutritional stress. Regarding expression of other AAT, only slight variations were observed. Most notably, female mice transcribed xCT (*slc7a11*) to a lesser extent than males ($P < 0.01$) (Figure 5D) but contrarily upregulated the expression of LAT2 ($P < 0.05$). This increase in LAT2 was possibly induced by the GCN2 pathway, as has been previously detected in cell culture[45]. AAT for glutamine did not vary between genotypes or sexes. SNAT3 and SNAT5 expression showed a general decrease during AP, SNAT2 a slight increase. Female LAT1-ko mice not only activated the mTOR pathway to a lesser extent and displayed pronounced sensitivity to nutritional stress, but they tended to show signs of defective autophagy. The well-established marker for autophagy, given as the ratio of microtubule-associated proteins 1A/1B light chain 3B II:I (LC3II:I)[46], was higher in female LAT1-ko compared to LAT1-wt mice ($P < 0.05$) (Figure 5E). The expression of mRNA coding for p62, a regulatory protein of autophagy[47], was increased during AP with higher levels in male mice (Figure 5F), but this did not translate to a change of p62 protein, which was equal among genotypes and sexes (Figure 5G) and suggested accumulation of the cargo protein in females.

Our results suggest that LAT1-ko mice activated the mTOR downstream target SK6 less effectively during the initial AP injury phase compared to LAT1-wt mice. Females more pronouncedly activated the starvation pathway GCN2, implied by increased phosphorylation of its downstream target eIF2α. They also showed evidence for dysfunctional autophagy, suggestive of an early metabolic adaptation depending on sex and the presence of LAT1.

LAT1-ko mice showed delayed recovery from acute pancreatitis with a more accentuated effect in females

As for wild-type mice, morphology, differentiation, and dedifferentiation markers, indicating the functional state of acinar cells, were analyzed in female and male LAT1-wt and LAT1-ko mice at the time points for which we observed maximum regenerative changes (day three) and almost normal

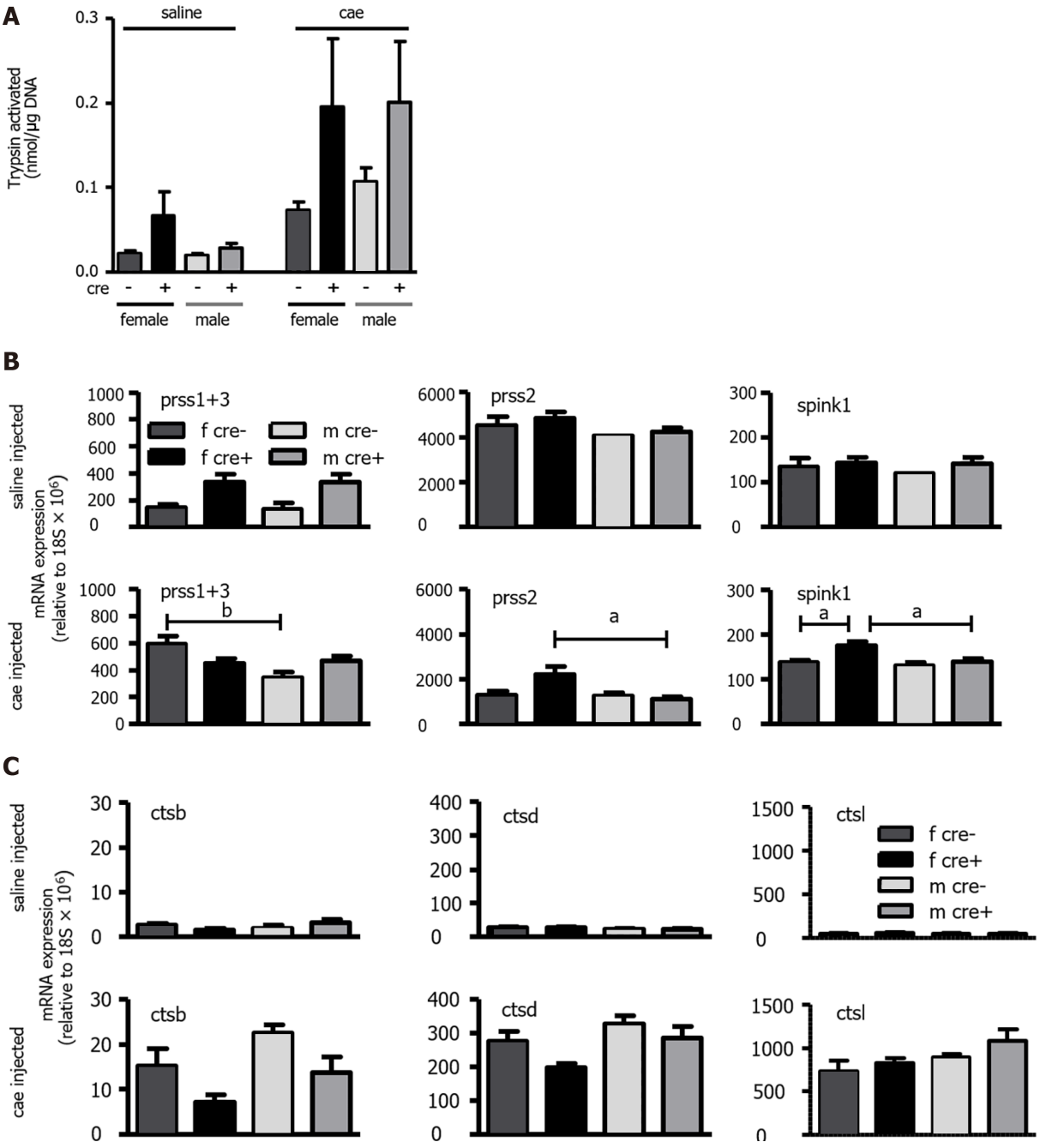

Figure 3 The trypsin activation observed in LAT1-ko mice had higher variability, and the expression of trypsinogens and cathepsins differed from LAT1-wt mice. A: Trypsin activation was observed in LAT1-wt and LAT1-ko mice 24 h after acute pancreatitis (AP) induction. The activity was measured using Boc-Q-A-R-MCA and expressed as nmol/µg DNA. Mean ± SEM, n = 3-7; B-C: The mRNA expression of trypsinogens, trypsin inhibitor, and cathepsins. The mRNA expressions of serine protease 1+3 (prss1+3) and serine protease 2 (prss2) along with serine peptidase inhibitor kazal type 1 (spink1) (B) and cathepsin B, D, and L (ctsb, ctsd, and ctsl) (C) were analyzed *via* qPCR and expressed relative to a housekeeping gene (18S × 10^6) in LAT1-wt and LAT1-ko mice. The upper panel depicts the mice that were injected with saline, and the lower panel shows the mice 24 h after AP induction. Mean ± SEM, n = 7-14. Statistical analysis was conducted with ANOVA and Bonferroni and compared, as indicated by the capped line. $^aP < 0.05$, $^bP < 0.01$, $^cP < 0.001$.

morphology (day seven) after induction of AP. Additionally, the body weights of the mice were controlled daily in this period. On day one of AP, the genotypes showed the same relative change of body weight but thereafter, LAT1-ko and especially female LAT1-ko lost more weight and did so more prolongedly (Figure 6A). Female LAT1-ko mice reached the highest weight loss on days three to five and still lagged their littermates on day seven.

As observed for wild-type mice three days after the induction of AP (Figure 1D), the presence of ADM could be detected in the tissue. Male LAT1-ko did not differ from male LAT1-wt mice, but female LAT1-ko had more extensive ADM areas than their LAT1-wt littermates (Figure 6B). By day seven, pancreatic tissue morphology in males of both genotypes and female LAT1-wt mice was almost restored, while female LAT1-ko mice still presented more areas with ADM.

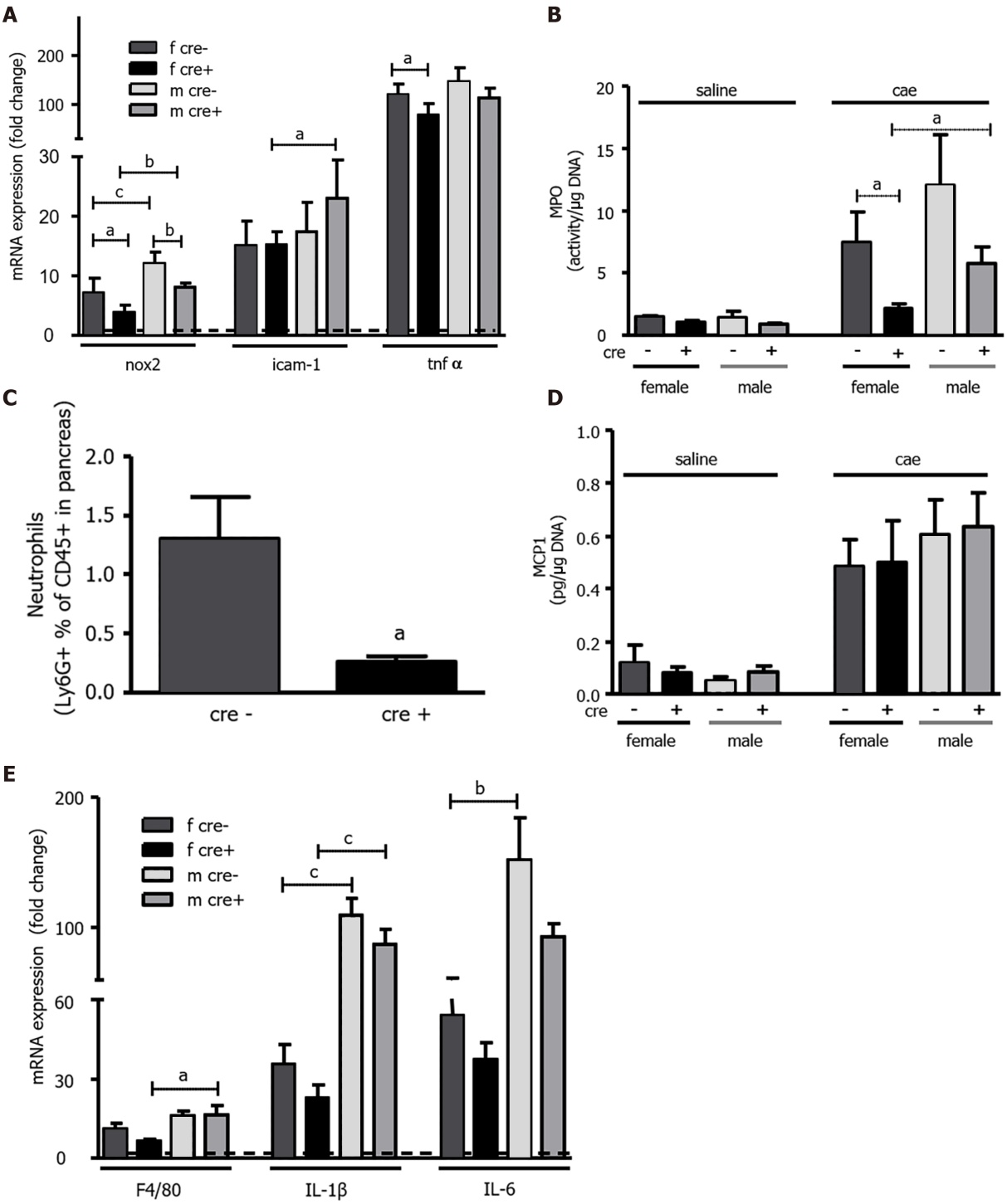

Figure 4 The number and activity of neutrophils in LAT1-ko mice was reduced, but the capacity to recruit macrophages was maintained. A-C: LAT1-ko mice recruited less neutrophils than LAT1-wt cre-mice. A: The mRNA expressions of NADPH oxidase 2 (nox2), tumor necrosis factor α (tnfα), and intercellular adhesion molecule 1 (icam-1) were analyzed *via* qPCR and expressed as a fold change relative to saline-injected controls 24 h after the onset of acute pancreatitis (AP). The line indicates the expression level of the control animals. Mean ± SEM, *n* = 4-7; B: Myeloperoxidase activity in LAT1-ko mice 24 h after saline or caerulein (cae) injection was expressed as activity/µg DNA. Mean ± SEM, *n* = 3-8; C: The lower number of neutrophils recruited was assessed by FACS analysis of the pancreas 24 h after the onset of AP. The results illustrate the ratio of Ly6G positive to CD45 positive cells. Mean ± SEM, *n* = 4-5. Statistical analysis was conducted with an unpaired, two-tailed t-test. $^{a}P < 0.05$; D-E: Recruitment of macrophages was equal in both genotypes, but female LAT1-ko mice exhibited a lower expression of macrophage marker and interleukins; D: Monocyte chemotactic protein 1 was equal between genotypes and sexes; this was measured by ELISA in the pancreas of saline or cae-injected mice and expressed as pg/µg DNA. Mean ± SEM, *n* = 3-8; E: Macrophage marker F4/80, interleukin 1β (IL-1β), and IL-6 were lower in female LAT1-ko when analyzed *via* qPCR and expressed as a fold change relative to saline-injected controls 24 h after the onset of AP. The line indicates the expression level of control animals. Mean ± SEM, *n* = 4-8. Statistical analysis was conducted with ANOVA and Bonferroni and then compared, as indicated by the capped line. $^{a}P < 0.05$, $^{b}P < 0.01$, $^{c}P < 0.001$.

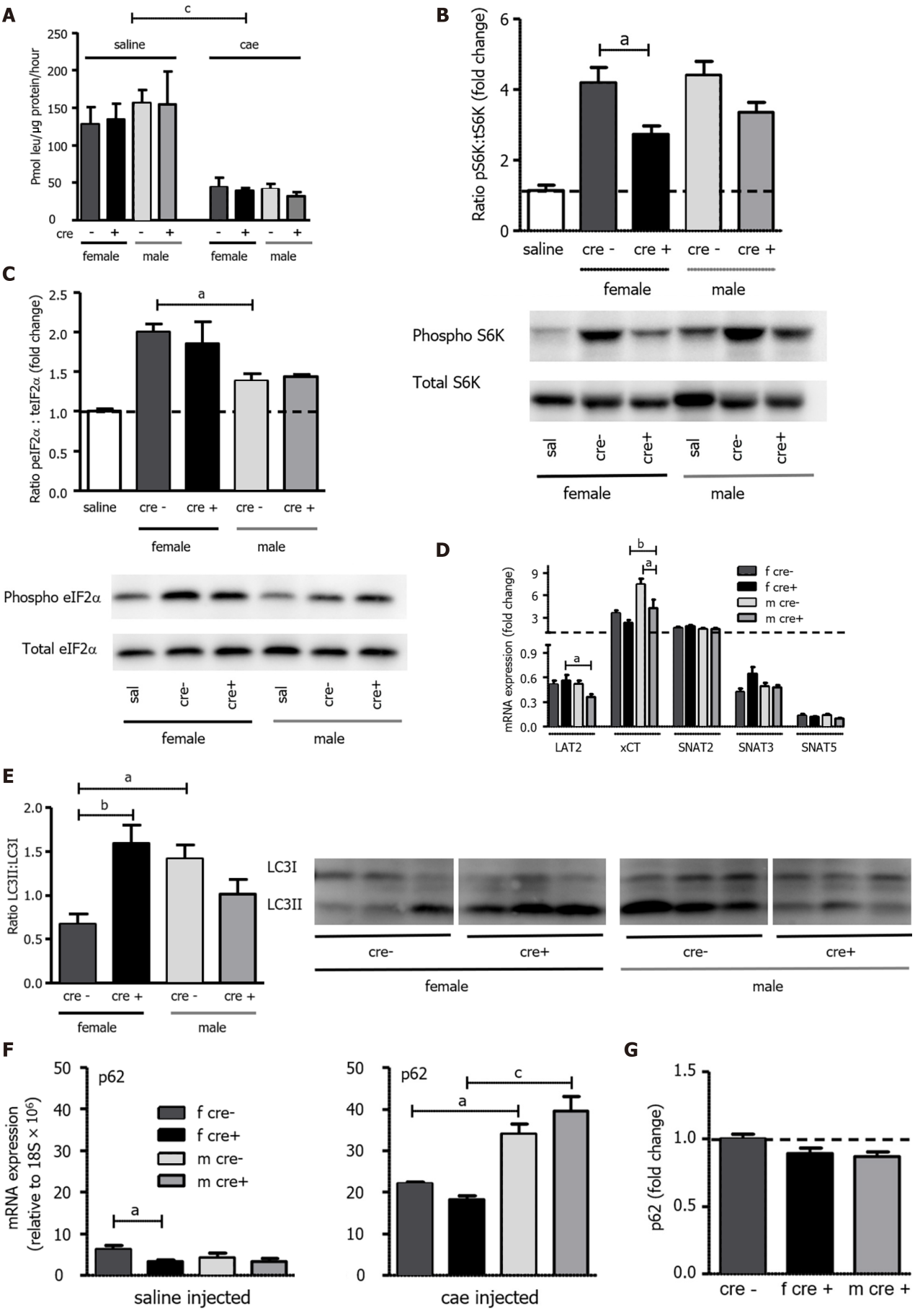

Figure 5 Protein synthesis, mammalian target of rapamycin, and general control nonderepressible 2 pathways as well as autophagy were

differently regulated upon knockout of LAT1. A: As measured by the incorporation of ^{3}H-leucine into total protein and expressed as pmol leu/mg protein/hour, protein synthesis was seen to decrease in both genotypes 24 h after the onset of acute pancreatitis (AP). Mean ± SEM, *n* = 3-8; B: The mammalian target of rapamycin (mTOR) downstream target S6 kinase (S6K) was activated to a lesser degree in female LAT1-ko mice. Phosphorylated and total S6K levels were determined with Western blotting (8% SDS-PAGE gel, cells' total lysates) 24 h after the onset of AP, and they showed a band at approximately 70 kDa. The results were expressed as a ratio of phosphorylated to total protein relative to the saline-injected controls; C: General control nonderepressible (GCN2) was more activated in females. The GCN2 downstream target eukaryotic-translation-initiating factor 2α (eIF2α) was analyzed *via* Western blotting (12% SDS-PAGE gel, cells' total lysates) 24 h after the onset of AP, and it exhibited a band at approximately 38 kDa. The results were expressed as ratio of phosphorylated to total protein, which was relative to the saline-injected controls. Mean ± SEM, *n* = 4; D: Variation of amino acid transporter expression after AP induction. The mRNA expression of LAT2 (*slc7a8*), xCT (*slc7a11*), SNAT2 (*slc38a2*), SNAT3 (*slc38a3*), and SNAT5 (*slc38a5*) was analyzed *via* qPCR and expressed as a fold change that was compared to saline-injected controls 24 h after the onset of AP. The line indicates the expression level of the control animals. Mean ± SEM, *n* = 5-8; E-G: Female LAT1-ko mice presented with enhanced markers for dysfunctional autophagy. E: The ratio of microtubule-associated protein 1A/1B-light chain 3 II (LC3II) to LC3I was higher in female LAT1-ko compared to female LAT1-wt. Moreover, the LC3II-to-LC3I ratio was examined using Western blotting (13.5% SDS-PAGE gel, cells' total lysates) 24 h after the onset of AP; a double band appeared at approximately 15 kDa. The upper band represents LC3I, and the lower band indicates LC3II. Mean ± SEM, *n* = 3-6; F-G: Male mice express more p62 mRNA, yet no more protein, than their female counterparts; F: The mRNA expression of p62 was analyzed *via* qPCR and expressed relative to a housekeeping gene (18S × 10^{6}) in LAT1-wt and LAT1-ko mice. The upper panel depicts the mice that were injected with saline, and the lower panel highlights the mice 24 h after AP induction. Mean ± SEM, *n* = 3-7; G: The p62 protein was analyzed with Western blotting (12% SDS-PAGE gel, cells' total lysates) 24 h after the onset of AP, and it exhibited a band at approximately 62 kDa. The results were expressed relative to β-tubulin and normalized in line with the LAT1-wt average indicated by the line. Mean ± SEM, *n* = 5-8. The statistical analysis was conducted by ANOVA and Bonferroni and then compared, as indicated by the capped line. *a* *P* < 0.05, *bP* < 0.01, *cP* < 0.001.

Overall, mRNA expression of genes characteristic for mature acinar cells analyzed on day three, rbpjl and mist1, was lower in female and male LAT1-ko mice than their LAT1-wt littermates. By day seven, expression in female LAT1-ko mice remained low, while female LAT1-wt mice and males from both genotypes had already restored expression levels (Figure 6C). This slower regeneration process in LAT1-ko mice, especially in females, was not caused by a difference in initial acinar cell death or following proliferation. Cleaved caspase, indicating apoptosis, was higher in acinar cells on day three for all genotypes and sexes compared to day seven, and the groups did not statistically differ between each other (Figure 6D). The phosphohistone 3 marker suggests that the proliferation of acinar cells was ongoing during the later time point of day seven, with only a tendency for female and male LAT1-ko mice to proliferate less than LAT1-wt animals early on day three (Figure 6E). Simultaneously, dedifferentiation markers sox9 and ck19 were elevated on days three and seven in both genotypes and sexes compared to saline-injected controls (Figure 6F). The early marker of dedifferentiation ck19 had already been elevated in both female and male LAT1-ko mice 24 h after AP induction (Figure 2G). On day three, male LAT1-wt and LAT1-ko mice behaved similarly, while female LAT1-ko reached higher ck19 levels than their LAT1-wt littermates, and these higher levels were maintained until day seven (Figure 6F). The described findings imply that pancreatic remodeling lasted beyond histologically determined normalization of the tissue and that LAT1 ablation in females worsened the condition.

Acinar cell function was assessed by amylase mRNA and protein expression as well as by total protein synthesis. Amylase levels were strongly reduced in LAT1-ko mice on day three, and female LAT1-ko showed still lower levels on day seven relative to female LAT1-wt mice (Figure 7A). Amylase levels were also decreased in LAT1-ko mice, as evidenced by immunofluorescence of the pancreas from mice of both sexes (Figure 7B). The quantification done by Western blotting confirmed the qualitative analysis through immunofluorescence, where we observed that female LAT1-ko mice expressed less amylase compared to LAT1-wt mice (Figure 7C). The observation that total protein synthesis in the tissue was still reduced three days after AP induction in both genotypes and female LAT1-ko mice remained significantly lower than saline-treated mice ($P < 0.05$) (Figure 7D) suggests that these lower amylase levels were due to a decrease in protein synthesis. Interestingly, the key regulators of protein synthesis mTOR (pS6) and GCN2 (eIF2α) pathways were equally activated in LAT1-wt and LAT1-ko mice. Ratios of phosphorylated to total S6K were not different from LAT1-wt (Figure 7E), and the same was observed for eIF2α, which had returned to control levels for both genotypes by day three (Figure 7F). The transport of amino acids into the cell is also crucial for protein synthesis. The expression of AAT was similar between the genotypes but differed between the sexes. In contrast to the early phase of AP (Figure 5D), SNAT3 expression remained lower in female compared to male mice on days three and seven (Figure 7G). The expression of xCT and SNAT2 were still elevated on day three, as we had observed after 24 h, but at this later time, xCT expression was similar in females and males. At the same time, LAT2 mRNA expression had almost returned to normal in all groups. SNAT5 expression, similar to amylase, remained reduced until the end of the experiment. Since we did not observe a difference in proliferation or acinar cell death, we analyzed the expression of markers for senescence and cell cycle arrest [48]. The gene encoding p21 (CDKN1A/CIP1), an inhibitor of cyclin-dependent kinases, was higher in female LAT1-ko mice ($P < 0.01$) three days after AP induction (Figure 7H). Another inhibitor of cyclin-dependent kinases, p27 (CDKN1B/KIP1), only tended to be elevated in female LAT1-ko mice seven days after AP induction. Lasting cell cycle inhibition might further indicate stalling recovery accentuated in female LAT1-ko mice.

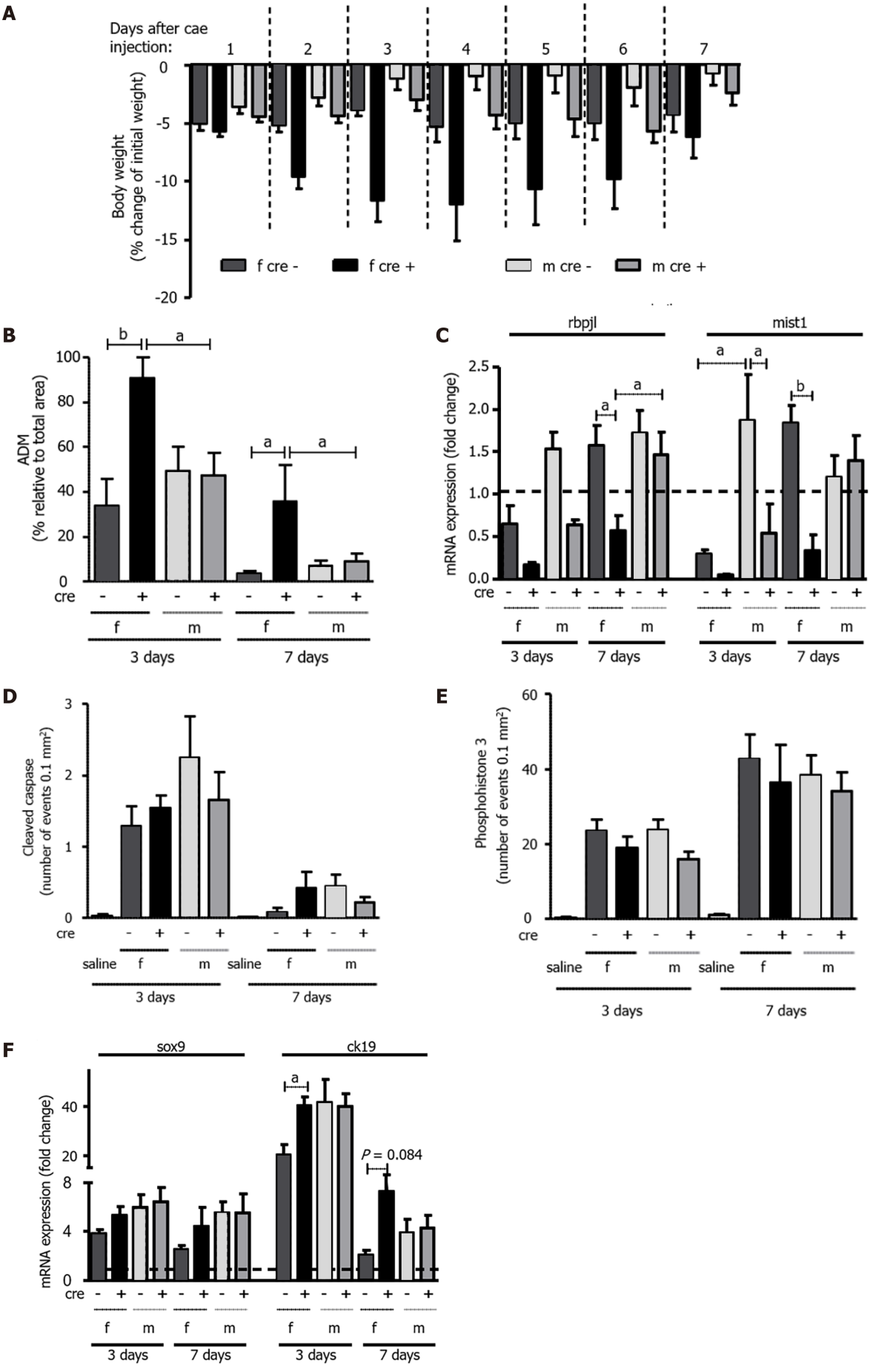

Figure 6 LAT1-ko mice showed a delayed recovery from acute pancreatitis, and the effect was more accentuated in females. A: Weight loss

in female LAT1-ko mice was more accentuated and prolonged compared to their LAT1-wt littermates. Their body weight was measured daily over a period of seven days after the caerulein injection, and it was then expressed as weight loss relative to their initial body weight. Mean ± SEM, n = 5-17; B: Acinar-to-ductal metaplasia (ADM) areas in female LAT1-ko mice were larger than in their littermates three and seven days after the onset of acute pancreatitis (AP). ADM structures were identified microscopically in the HE stains and expressed as a percentage that was relative to the total area of the pancreas. Mean ± SEM, n = 5-9; C: Markers of pancreas-specific differentiation were lower in female LAT1-ko mice up to seven days after the onset of AP. Meanwhile, the mRNA expression of recombining the binding protein suppressor of hairless-like protein (rbpjl) and basic helix-loop-helix family member A15 (mist1) was analyzed *via* qPCR, expressed as a fold change, and then compared to saline-injected controls three and seven days after the onset of AP. The line indicates the expression level found in the control animals. Mean ± SEM, n = 3-5; D-E: Apoptosis and proliferation did not differ between the groups with AP, as demonstrated by immunohistochemistry analyses of D: cleaved caspase and E: phosphohistone 3, respectively. The results were expressed according to the number of events in acinar cells per 0.1 mm^2. Mean ± SEM, n = 5-9; F: The expression level of genes that are characteristic of dedifferentiation was elevated in female LAT1-ko mice up to day seven. Meanwhile, the mRNA expression of SRY-box transcription factor 9 (sox9) and cytokeratin 19 (ck19) was determined *via* qPCR and expressed as a fold change, which was compared to saline-injected controls three and seven days after the onset of AP. The line indicates the expression level of the control animals. Mean ± SEM, n = 3-5. Statistical analysis was conducted with ANOVA and Bonferroni and then compared, as indicated by the capped line. $^{a}P < 0.05$, $^{b}P < 0.01$, $^{c}P < 0.001$.

This set of experiments suggests that LAT1-ko mice were delayed in initiating differentiation, recovering protein synthesis capacity, and restoring body weight compared to their LAT1-wt littermates. Also, at three to seven days, female LAT1-ko mice presented disrupted regeneration steps compared to male littermates.

Female LAT1-ko mice presented higher fibrosis marker expression and microscopical evidence of fibrosis compared to their wild-type littermates

The presence of fibrosis alters the morphological characteristics of the tissue but can also influence cellular interaction and slower regeneration processes after AP[8]. To verify if the ablation of LAT1 in LAT1-ko mice could modify regeneration by influencing the generation of fibrosis, we assessed the presence of fibrosis indicators directly by histological and immunohistological analysis as well as by mRNA expression and protein levels of fibrosis markers. The Masson's trichrome histological staining showed noticeable aggregation of fibrotic tissue throughout the pancreas of LAT1-ko females (Figure 8A). The activation of pancreatic stellate cells (PSC) was evidenced by the deposition of SMA with immunofluorescence (Figure 8B) and Western blotting analysis (Figure 8C) as well as a decrease in vimentin ($P < 0.05$) (Figure 8D). Both confirmed the higher presence of markers characteristic for activated PSC in female LAT1-ko mice. Female LAT1-ko mice exhibited a higher presence of collagen mRNA on day three and tended to express more transforming growth factor β (tgfβ) than their male littermates on days three and seven (Figure 8E). Macrophages have been previously identified to influence the restoration of homeostasis[49]. In females, the expression of macrophage marker F4/80 and CD206/MRC1 indicative of type 2 macrophages did not differ from males three days after AP (Figure 8E) but had a slight tendency to be lower, while the anti-inflammatory marker IL-10 was not enhanced in females or males. Interestingly, seven days after AP, all the genes related to fibrosis remained elevated in female LAT1-ko compared to male mice. Altogether, these results propose that LAT1-ko mice developed more fibrosis and regenerated more slowly, with accentuated manifestation in females.

DISCUSSION

A change in the expression of AAT during the early phase of AP was shown in our previous work[17]. To investigate the significance of this observation, we analyzed the course of AP from the early phase to regeneration in the present study, focusing on the role of the AAT LAT1 (*slc7a5*). We examined the expression of different AAT, protein synthesis and upstream regulatory mechanisms, markers of injury, proliferation, and fibrosis. We observed a delay in the recovery phase of LAT1-ko mice compared to LAT1-wt after AP induction. We here discuss the possible influences of LAT1 expression on these mechanisms in particular and in AP disease progression in general and the limitations and possible follow-ups of this study.

LAT1 ablation was not compensated by other amino acid transporters in a global LAT1 knockout mouse model

AATs are responsible for the continuous influx of amino acids used for protein synthesis in acinar cells [50] and can also act upstream of cellular pathways controlling cell survival and proliferation[51]. LAT1 expression persisted during the first 24 h of AP when the differentiation markers recombining binding protein suppressor of hairless-like protein (rbpjl) and basic helix-loop-helix family member A15 (mist1) were reduced, and the early dedifferentiation marker ck19 was increased. LAT1 was detected on membranes of acinar cells and ADM, suggesting its presence in the remaining dedifferentiated acinar cells may support cell survival. The knockout of LAT1 was efficient until the end of the experiment and

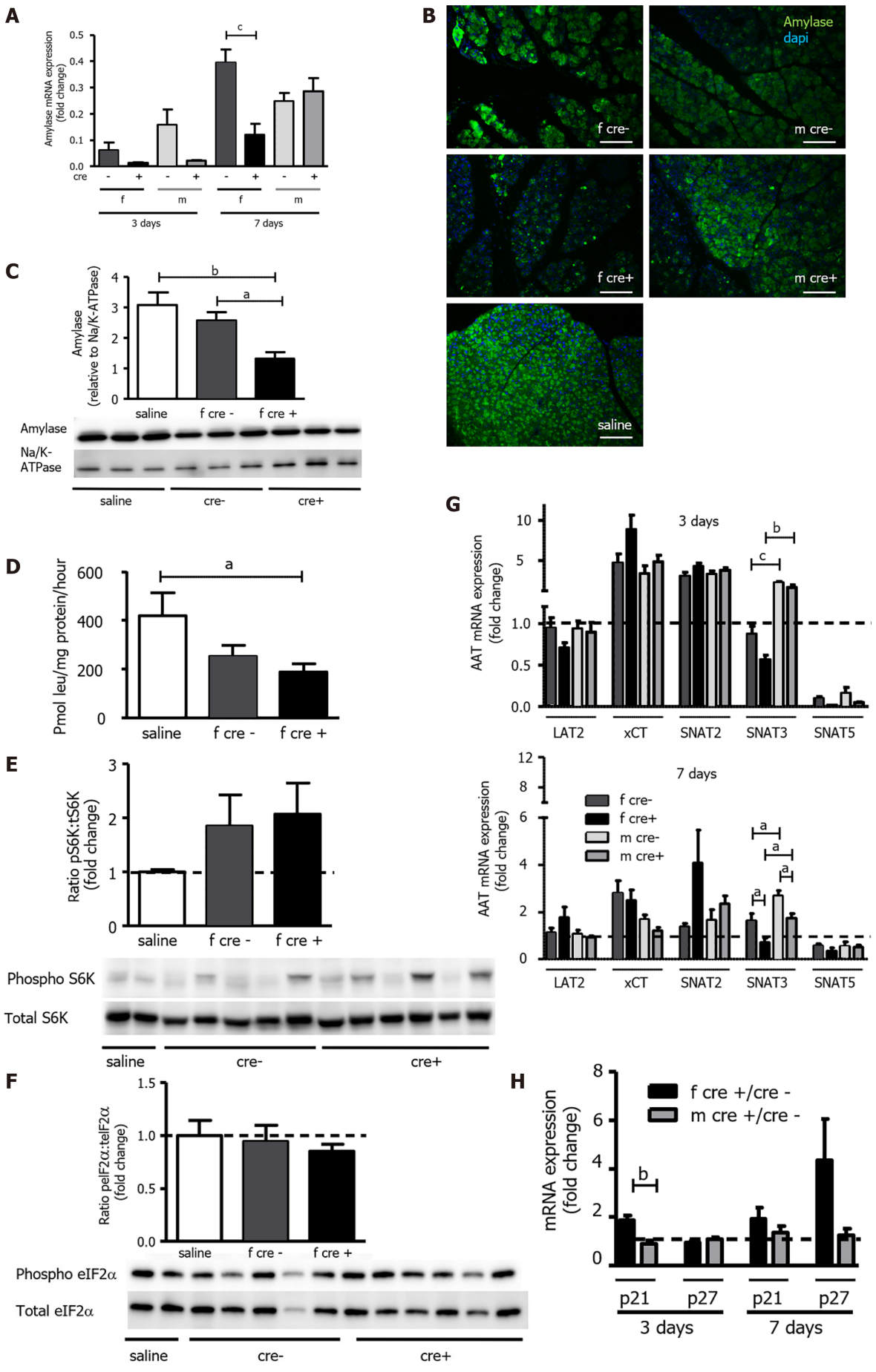

Figure 7 Functional recovery of acinar cells was delayed in LAT1-ko mice after injury. A-C: Amylase mRNA and protein levels were reduced in

female LAT1-ko mice. A: The mRNA of amylase was examined *via* qPCR and expressed as a fold change; subsequently, this value was compared to those relating to the saline-injected controls three and seven days after the onset of acute pancreatitis (AP). Mean ± SEM, *n* = 45. Subsequently, statistical analysis was conducted with ANOVA and Bonferroni and then compared, as indicated by the capped line. *cP* < 0.001; B: Decreased amylase expression could also be evidenced by reduced signal intensity in immunofluorescence three days after AP induction. The paraffin-embedded mouse pancreas was stained for amylase (green), and the nuclei were stained in blue (dapi). The bar length corresponds to 100 μm; C: Amylase protein was analyzed with Western blotting (10% SDS-PAGE gel, cells' total lysates) three days after the onset of AP; it exhibited a band at approximately 60 kDa. The results were expressed relative to Na/K-ATPase; D: LAT1-ko mice showed lower protein synthesis compared to the saline-injected controls, as measured by the incorporation of ^{3}H-leucine into total protein and expressed as pmol leu/mg protein/hour three days after the onset of AP in female mice. Mean ± SEM, *n* = 3-8. Statistical analysis was conducted with ANOVA and Bonferroni and then compared, as indicated by the capped line. *aP* < 0.05; E-F: Mammalian target of rapamycin was increased, and the general control nonderepressible 2 (GCN2) pathway was not activated in LAT1-ko mice three days after AP; E: Phosphorylated and total S6K levels were determined with Western blotting (8% SDS-PAGE gel, cells' total lysates) three days after the onset of AP; there was a band at approximately 70 kDa. The results were expressed as a ratio of phosphorylated to total protein relative to the saline-injected controls; F: GCN2's downstream target eukaryotic-translation-initiation factor 2α was analyzed using Western blotting (12% SDS-PAGE gel, cells' total lysates) three days after the onset of AP, and a band appeared at approximately 38 kDa. The results were expressed as a ratio of phosphorylated to total protein relative to the saline-injected controls. Mean ± SEM, *n* = 5-6; G: The expression of SNAT3 was lower in female mice until seven days after the onset of AP. The mRNA expression of LAT2 (*slc7a8*), xCT (*slc7a11*), SNAT2 (*slc38a2*), SNAT3 (*slc38a3*), and SNAT5 (*slc38a5*) was analyzed *via* qPCR and expressed as a fold change in comparison with saline-injected controls three and seven days after the onset of AP. The line indicates the expression level of the control animals. Mean ± SEM, *n* = 5-10. Statistical analysis was conducted with ANOVA and Bonferroni and then compared, as indicated by the capped line. *aP* < 0.05, *bP* < 0.01, *cP* < 0.001; H: Expression of senescence markers was more accentuated in female LAT1-ko mice up until seven days after the onset of AP. The mRNA levels of p21 and p27 were analyzed *via* qPCR and expressed as a fold change, which was compared to the LAT1-wt group three and seven days after the onset of AP. The line indicates the expression level of the LAT1-wt animals. Mean ± SEM, *n* = 5. Statistical analysis was conducted *via* an unpaired, two-tailed t-test. As indicated by the capped line, a comparison was then made. *bP* < 0.01.

did not cause compensatory upregulation of other AAT. LAT2 (*slc7a8*), especially, which has a similar substrate specificity as LAT1[52] and the capacity to activate mammalian target of rapamycin (mTOR) signaling[53], was not upregulated in acinar cells. This stands in contrast to constitutive muscle-specific ablation of LAT1 (*MCK-cre slc7a5*), where LAT2 mRNA was upregulated in muscle fibers[29]. We also investigated the potential effect of LAT2 deficiency on LAT1 expression in the pancreas, but no direct compensation was detected (data not shown). The expression of other AAT, which we previously described to be modulated during early AP induction[17], was neither influenced by LAT1 ablation nor the treatment with tamoxifen. To conclude, the inducible LAT1 knockout mouse model appeared to be adequate to study the role of LAT1 in the different phases of AP without compensation of other transporters in the pancreas.

LAT1 knockout mice sustained a similar injury to the wild-type 24 h after acute pancreatitis induction

The intrapancreatic activation of trypsinogen to trypsin has been suggested as an early event during AP and is used as a marker for the extent of injury[5]. In our study, both genotypes presented a similar mean increase of intrapancreatic trypsin activity, but the values in knockout mice were more variable than in wild-types. Intrapancreatic activation of trypsinogen is controlled by the interplay of cathepsin B, cathepsin D, and cathepsin L[40,54,55] localized in the lysosomes of acinar cells and also released by leukocytes[41]. The specific ablation of cathepsin D in leukocytes has a pronounced effect on trypsinogen activation during AP, suggesting the reduced neutrophil recruitment we observed in LAT1-ko mice might have contributed to the variability in trypsin activation. Nonetheless, mice with deficient neutrophil recruitment can develop AP and only present a stalled increase of plasma lipase[56]. In our model, the reduced number of neutrophils did not delay or depress plasma injury markers. Plasma levels of lipase and amylase were equally changed in both genotypes and confirm that LAT1 ablation did not culminate in less severe injury. We describe for the first time that LAT1 expression affects leukocyte recruitment, while the importance of LAT1 expression for the activation of macrophages[57, 58] and T-cells[22] has already been recognized.

Further, we did not observe a variation of macrophage markers between the genotypes, but a sex difference appeared. Female mice presented diminished expression of macrophage markers in the early injury phase. Moreover, mRNA for IL-1β and IL-6 in female LAT1-ko mice was reduced 24 h after AP induction. This possibly corresponded with a lower number of monocytes and the missing transporter activity on these cells. Yet, LAT1 genotypes displayed the same indicators of AP, implying that the disease developed in the presence of fewer neutrophils and macrophages. As we applied a whole-body knockout, the effects of immune cells' LAT1 expression on inflammatory processes during AP overlap with the significance of this AAT in acinar cells. We envisage future studies to focus on the impact of LAT1 in pancreatic acinar cells with a conditional inducible knockout for LAT1, specifically in these secretory cells.

LAT1 ablation interfered with the mTOR pathway and regeneration of acinar cells in the early injury phase 24 h after acute pancreatitis induction

Another established characteristic of AP is the reduced pancreatic function evidenced by a decreased protein synthesis[43]. In acinar cells, the synthesis of digestive enzymes is regulated through the mTOR pathway[59] and amino acid availability[60]. The initial inhibition of the mTOR pathway, decreased

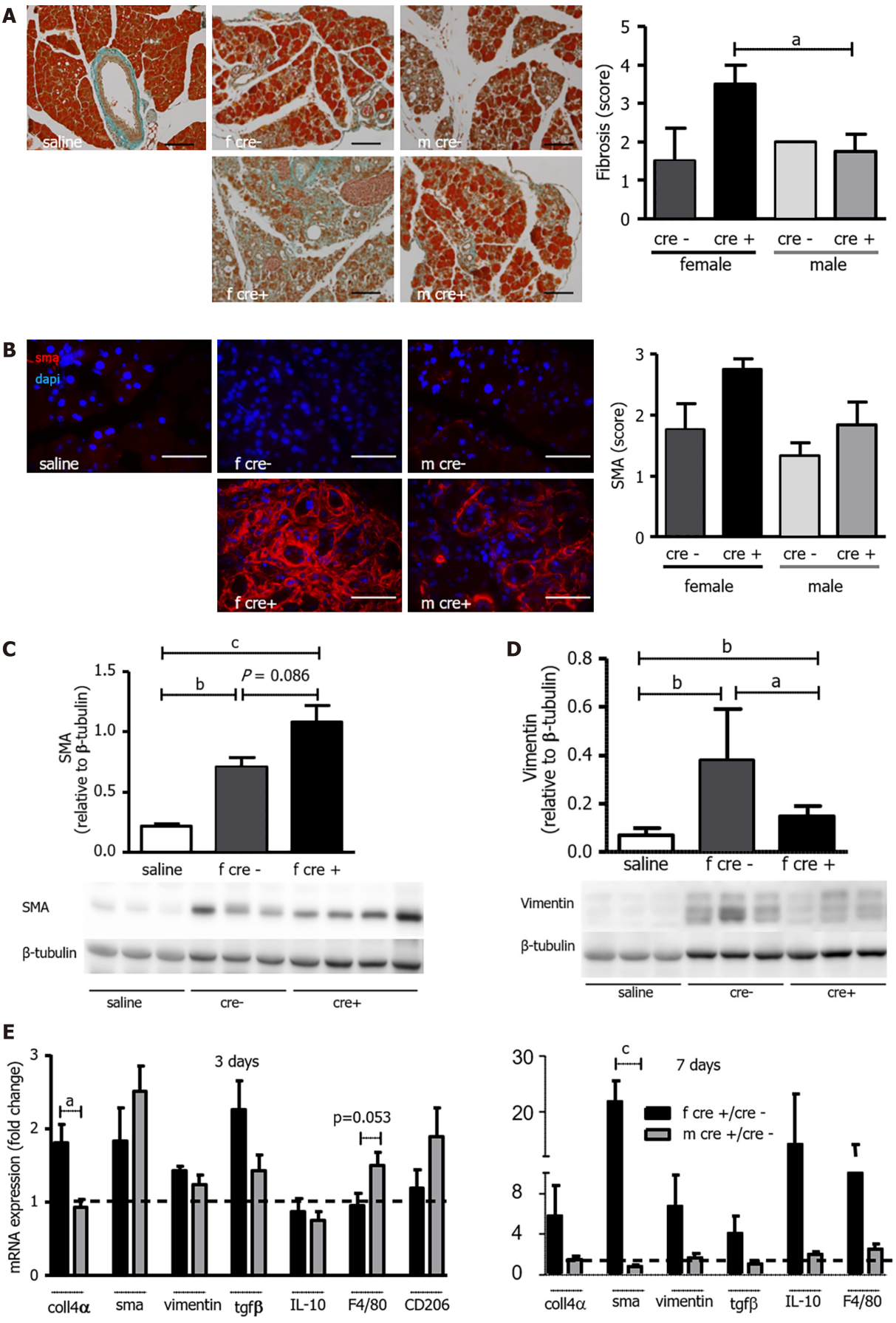

Figure 8 Female LAT1-ko mice presented with higher levels of fibrosis and expression of markers thereof. A: Female LAT1-ko mice presented with larger areas of fibrosis. Masson's trichrome staining (left) and quantification (right) of fibrosis in the pancreas three days after the onset of acute pancreatitis (AP).

A score from 0 to 5 was attributed to each section in a blinded fashion, which was dependent on the extent of the fibrosis. The Bar length corresponds to 100 μm. Mean ± SEM, *n* = 4-6. Statistical analysis was conducted with ANOVA and Bonferroni and then compared, as indicated by the capped line. *aP* < 0.05; B-D: Female LAT1-ko mice exhibited enhanced activation of pancreatic stellate cells (PSC) compared to their littermates; B: Immunohistochemistry (left) and quantification (right) for smooth muscle actin (SMA) in the pancreas three days after the onset of AP. A score from 0 to 3 was attributed to each section in a blinded fashion depending on the signal intensity of the SMA staining. The paraffin-embedded mouse pancreas was stained for SMA (red) and the nuclei were stained in blue (dapi). The bar length corresponds to 50 μm. Mean ± SEM, *n* = 5; C: SMA that was indicative of activated PSC was also analyzed with Western blotting (12% SDS-PAGE gel, cells' total lysates from female mice) three days after the onset of AP; this process led to a band being exhibited at approximately 42 kDa. The results were expressed relative to β-tubulin. Mean ± SEM, *n* = 3-6. Statistical analysis was conducted by ANOVA and Bonferroni and then compared, as indicated by the capped line. *bP* < 0.01, *cP* < 0.001; D: The marker for non-activated stellate cells of vimentin was less expressed in the female LAT1-ko mice. Vimentin was also analyzed by Western blotting (10% SDS-PAGE gel, cells' total lysates from female mice) three days after the onset of AP and showed a band at approximately 57 kDa. The results were expressed relative to β-tubulin. Mean ± SEM, *n* = 3. Statistical analysis was conducted with ANOVA and Bonferroni and then compared, as indicated by the capped line. *aP* < 0.05; E: Female LAT1-ko mice showed an elevated expression of markers for fibrosis and similar markers for macrophages when compared to male mice on day three. The mRNA levels of collagen 4α (coll4α), SMA, vimentin, transforming growth factor β, interleukin 10, F4/80, and CD206 were analyzed *via* qPCR and expressed as a fold change in comparison with LAT1-wt mice three and seven days after the onset of AP. The line indicates the expression level of LAT1-wt animals. Mean ± SEM, *n* = 5. Statistical analysis was conducted *via* an unpaired, two-tailed *t*-test, and a comparison was then made, as indicated by the capped line. *aP* < 0.05, *cP* < 0.001.

protein synthesis, and activation of autophagy have been shown as crucial for the dedifferentiation process. The following reactivation of the mTOR pathway allows cells to proliferate and differentiate and supports tissue repair[15]. In our model, mTOR reactivation 24 h after AP induction was less pronounced in LAT1-ko mice. As shown in other cell types, LAT1 works as a sensor for extracellular amino acid availability and upstream regulator of mTOR[25,58]. LAT1 ablation can inhibit this pathway [61], and our results suggest that LAT1 knockout partially blocked the reactivation of mTOR. Moreover, the GCN2 intracellular sensing pathway for amino acid availability was found enhanced after AP. GCN2 decreases general protein synthesis to reduce energy expenditure and induces upregulation of genes such as AAT (LAT2, xCT, SNAT3) and stress markers (activating transcription factor 4 (ATF4), CHOP, CHAC1)[45]. The induction of the starvation pathway *via* GCN2 was activated in both genotypes and was higher in female mice. More than that, we found certain sex differences between the regulation of GCN2 downstream genes during the early injury phase 24 h following the onset of AP. While SNAT3 and ATF4, C/EBP homologous protein (CHOP), and Glutathione Specific Gamma-Glutamylcyclotransferase 1 (CHAC1) (data not shown) behaved equally for all genotypes and sexes, LAT2 and xCT expression varied between female and male mice. These results imply that GCN2 downstream regulation in acinar cells is sex-dependent, as previously observed for mTOR[62]. Besides sex, distinctive regulation of the mTOR pathway depending on age and tissue type has been found in mice. Notably, in the liver and heart, mTOR is more enhanced in fasted female than male mice, while activation in muscle and fat revealed no sex difference. A better understanding of mTOR and GCN2 pathway regulation in the pancreas according to sex and age may be helpful to comprehend regeneration processes in different situations and influences of other components such as AAT.

Another source of amino acids during starvation arises through the activation of autophagy. Autophagy plays an important role during regeneration[15], and inhibited or defective autophagy can eventually delay this process[63]. We observed indicators of abnormally large autolysosomes (high LC3II/LC3I ratio) in female LAT1-ko mice and accumulation of cargo protein (p62) characteristic of defective autophagy in AP[64,65]. These results suggest that female LAT1-ko mice especially did not manage to compensate for the less activated mTOR pathway by increasing the catabolism of pre-existing proteins. To summarize, LAT1-ko mice showed blunted activation of the mTOR pathway and enhanced amino acid starvation accentuated in female mice with indicators of dysfunctional autophagy. Even though AP injury itself was not more severe, the ablation of LAT1 weakened the initial mechanisms that sustain regeneration in acinar cells.

Ablation of LAT1 leads to slower regeneration identified three to seven days after acute pancreatitis induction

We followed up for seven days to evaluate if the initial blunted metabolic adaptation observed in LAT1-ko mice influenced later regeneration steps. LAT1-ko mice, particularly females, presented accentuated weight loss and recovered more slowly than their LAT1-wt littermates. The knockout of LAT1 was induced by tamoxifen, which is known to change fat composition in female but not in male mice[66]. The enhanced weight loss in female LAT1-ko mice cannot be explained by tamoxifen alone since female LAT1-wt were likewise treated with the drug and did not present the same sustained weight loss. In addition to tamoxifen effects, the reduction in digestibility and absorption of nutrients generally taking place during AP[67] might have accounted for the more severe weight loss in females.

When it comes to functional pancreatic integrity, the transcription factor mist1 warrants further attention. Mist1 is highly expressed in a mature pancreas and governs digestive enzymes[68]. In rodents, transcription of digestive enzymes and differentiation marker mist1 decreases after AP induction[9,20]. Upon AP, mist1 expression is temporarily silenced to allow functional reduction, dedifferentiation, proliferation, and regeneration to occur[10]. Indeed, female LAT1-ko mice did not

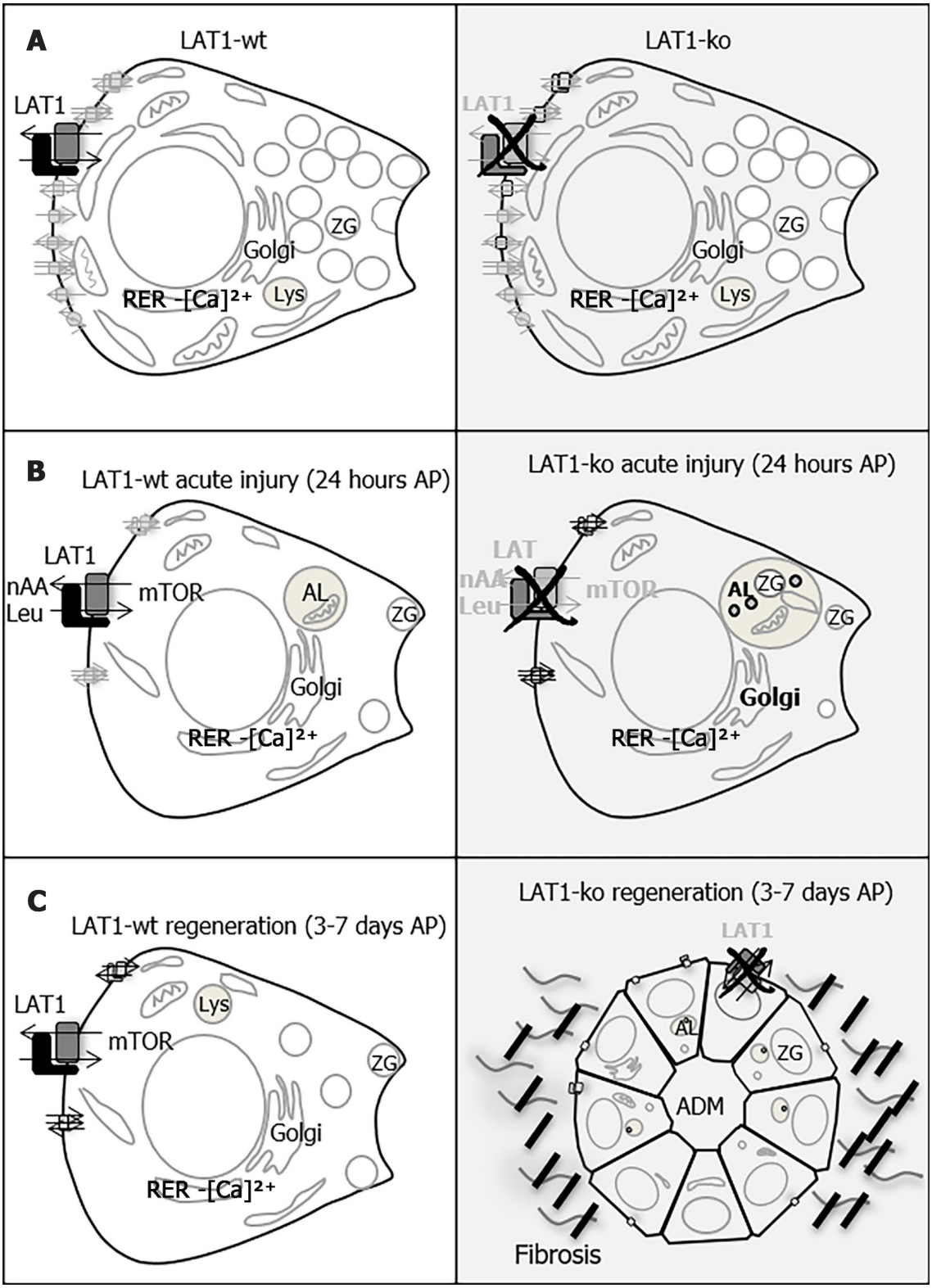

Figure 9 LAT1 ablation affects the initial metabolic adaptation that is necessary for the efficient repair after acute pancreatitis. Acinar cells have a pyramidal shape and display a typical secretory machinery with a well-developed rough endoplasmic reticulum (RER) and Golgi apparatus (Golgi), which are localized to the perinuclear region, as well as lysosomes (Lys). In the apical region, digestive enzymes are stored in zymogen granules (ZG). A: Amino acid transporters (AAT) are expressed on the basolateral membrane of acinar cells and are responsible for the transportation of amino acids into the cells to maintain the synthesis of secreted enzymes; this is so they can be used as an energy source and to guarantee cell growth and regeneration after injury. LAT1 exchanges leucine (Leu) with other neutral amino acids (nAA), and the amino acid flow acts as an upstream regulator of the mammalian target of rapamycin (mTOR) pathway, which regulates protein synthesis and enables cell differentiation/survival. Morphology, enzyme expression, and other AAT expressions did not differ between healthy LAT1 wild-type (LAT1-wt, white, left-hand panel) and healthy LAT1 knockout (LAT1-ko, gray, right-hand panel) mice over the period observed in this study; B: During the early phase of AP, the remaining acinar cells entered a metabolic arrest, dedifferentiated, and temporarily reduced their secretory phenotype. An increase in autophagy (AL, autolysosome), followed by the re-activation of the mTOR pathway is decisive for the later steps of regeneration. LAT1 expression is maintained on

acinar cells of LAT1-wt mice in this early phase, and it plays a role in the reactivation of mTOR. In LAT1-ko mice, the massive reduction of secretory enzyme expression was accompanied by markers of defective autophagy and a less-efficient activation of mTOR; C: Three days after the initial injury, LAT1-ko acinar cells were less differentiated and presented more areas of acinar-to-ductal metaplasia (ADM), expressed less secretory enzymes, and showed increased fibrosis. The delayed regeneration observed in acinar cells lacking LAT1 suggests that this occurred as a result of the improperly activated early metabolic response after injury.

recover mist1 expression until the end of the experiment. In agreement with the lower expression of differentiation markers, the expression of amylase indicative of pancreatic function was reduced compared to their female and male littermates. In humans, exocrine pancreatic insufficiency can develop even after milder episodes of AP, increasing the risk of malnutrition and malabsorption for prolonged periods after AP[69]. This process might have been amplified in female mice, where the ablation of LAT1 slowed the recovery of exocrine function after AP induction.

Mist1 is also an upstream regulator of the AAT SNAT5[9,70]. SNAT5 behaved as amylase and did not regain its normal expression level until the end of the experiment. This finding suggests that SNAT5 may play a role in protein synthesis, although knockout of this AAT did not induce changes in pancreas function or morphology of healthy mice[71]. In contrast to SNAT5, the AAT xCT and SNAT2 were still overexpressed three days after AP induction in all groups. They are known to be influenced by different cellular stress pathways. xCT expression is modulated by the master regulator of oxidative stress nuclear factor erythroid 2-related factor 2 (nrf2)[72], which was likewise elevated in all groups (data not shown). SNAT2 expression is controlled by the GCN2-ATF4 starvation pathway[73], which was increased in the earlier stages during AP. Interestingly, SNAT3 was overexpressed three days after AP induction in our model as well, but only in male mice. Since SNAT3 is influenced by androgens[74], the increased expression of this transporter might have an endocrine cause. Our results show that the expression of AAT during the regeneration phase varied, as observed for the early injury after AP induction. Thus, the regulation of AAT seems to be multifactorial, and a certain degree of sexual dimorphism in amino acid metabolism is present, as observed in the liver[75].

Further, mist1 directly controls the senescence marker p21 in acinar cells[76], which was enhanced during AP, especially in female LAT1-ko up to seven days. Overexpression of p21 has been correlated with the development of fibrosis[77], which can occur transiently during tissue regeneration and prolong recovery from AP[78,79]. Fibrosis is usually accompanied by the activation of PSC and the deposition of extracellular matrix (ECM) proteins[80]. Accordingly, we observed that female LAT1-ko mice presented higher deposition of ECM and showed higher activation of PSC, despite tamoxifen treatment. Tamoxifen is known to reduce PSC activation in the liver[81] and pancreas[82], especially in males[83]. Cae- and saline-injected mice from both genotypes and sexes were treated with tamoxifen to minimize the outcome in our setup. Thus, tamoxifen alone did not account for the difference in PSC activation and ECM synthesis. This implies that the delayed recovery in female mice was mainly caused by LAT1 ablation.

The maintenance or resolution of fibrosis is also regulated by metalloproteases released by specific populations of macrophages[49]. Throughout the phases of acute inflammation to recovery, the macrophage profile changes from M1- to M2-like, with M1 active during the early injury and M2 playing a role during regeneration. The ablation of macrophages in the early injury phase protects the tissue, while the ablation of macrophages three days after injury delays regeneration[84]. Interestingly, female LAT1-ko mice exhibited indicators of fewer macrophages in the tissue during the initial injury phase but partially recovered macrophage markers by day three. Moreover, the marker for M2 macrophages did not differ between LAT1-ko females and males. This implies that macrophages were not solely responsible for the increased ECM deposition in female LAT1-ko.

Finally, although we know that acinar cells can activate PSC[85], it remains unexplored whether changes in acinar cells' amino acid metabolism can influence the microenvironment and promote PSC activation or ECM deposition. Insight into these mechanisms might advance the understanding of pancreatic disease with future clinical implications.

CONCLUSION

Altogether, we showed that the ablation of LAT1 (*slc7a5*) affects the initial metabolic adaptation necessary for the efficient repair after AP, finally delaying regeneration and enhancing fibrosis (Figure 9A-C). This study revealed important elements for a better understanding of repair processes in pancreatic tissue after AP. Equally significant, with gender medicine evolving in diverse fields[86], including in the clinical setting of AP[87,88], we suggest that a higher consideration of sex differences with separate evaluation of female and male specimens should also be established in pre-clinical studies of AP.

ARTICLE HIGHLIGHTS

Research background

As a highly metabolically active organ, the pancreas depends on a constant supply of amino acids to synthesize digestive enzymes and for use as an energy source. This multifunctionality is reflected in the broad range of expressed amino acid transporters (AAT). Furthermore, after acute injury, the organ is capable of regeneration. Following acute pancreatitis (AP), acinar cells change their metabolic and functional state, initially dedifferentiating, increasing proliferation, and finally restoring their secretory function. AAT that are expressed in pancreatic acinar cells might play an additional role, which involves controlling the transcription of secreted enzymes and thus influencing the course of pancreatic disease and regeneration. LAT1 works as a sensor for extracellular amino acid availability and is an upstream regulator of the mammalian target of rapamycin pathway. This transporter is overexpressed in highly proliferative cells. Additionally, our previous study showed that LAT1 is expressed in acinar cells and that LAT1 expression in the early phase of AP is maintained in a different way to other AAT.

Research motivation

Lasting pancreatic disease is often detrimental to the quality and duration of life. Despite the high incidence of AP, there are no specific treatments, yet understanding pathophysiological processes is a crucial part of enabling future studies on preventative and therapeutic options. The role of AAT in this process is not comprehensively understood. Their pattern of expression may indicate that necessary metabolic adjustments are needed to meet the requirements for regeneration and reconstitution of function, which could be used as a supportive intervention during treatment.

Research objectives

The focus of the present study was to analyze metabolic alterations in the pancreas during acute inflammation by concentrating on the role of LAT1. The degree of initial injury as well as the course of regeneration were studied to investigate the significance of LAT1.

Research methods

To investigate the role of LAT1, an inducible knockout mouse model was applied, and the course of caerulein- (cae-) induced AP was studied in line with the phases of injury through to regeneration. Moreover, we analyzed the function of acinar cells and several markers of dedifferentiation and metabolic pathways.

Research results

The absence of LAT1 did not cause more severe injury during AP, but it did alter early metabolic adaptation. Consequently, differentiation and the function of acinar cells in LAT1 knockout mice were reduced, which influenced the regeneration phase. A sex-related difference was also revealed: female mice sustained more pronounced cell dedifferentiation and fibrosis.

Research conclusions

LAT1 supports the regeneration of pancreatic acinar cells after AP *via* metabolic adaptation, influencing their differentiation as well as their recovery of function and phenotype. The knocking out of LAT1 had a more accentuated effect in female mice, suggesting that a sex-dependent dimorphism in AAT is present in the pancreas.

Research perspectives

Future studies should focus on the role of AAT and metabolic pathways in acinar cells by using conditional knockout models. An acinar-cell conditional knockout or overexpressing mouse model will allow us to analyze the effect of AAT, specifically in pancreatic cells, without affecting their expression in immune cells, which play an important role in the development of AP. Additionally, induction methods other than tamoxifen should be tried, and sex-dependent differences as well as the influence of age should be further considered. These models will enable a better understanding of the metabolic mechanisms, guaranteeing the survival of acinar cells after different insults.

ACKNOWLEDGEMENTS

The authors cordially thank Brigitte Herzog and the Zurich Integrative Rodent Physiology Facility, in particular Petra Seebeck and Svende Pfundstein, for their support with the animal experiments. We also thank Birgit R Z'graggen and Peter Hunziker for assisting with the amino acid measurements at the Functional Genomics Center Zurich (FGCZ). Additionally, we are grateful to Josep M Rodríguez from the Institute of Veterinary Pathology for his help with the slide scanner.

FOOTNOTES

Author contributions: Camargo SM, Poncet N, and Hagen CM designed and coordinated the study; Hagen CM, Roth E, Reding T, Gupta A, Pellegrini G, and Camargo SM performed the experiments, acquired and analyzed data; Hagen CM, Reding T, Verrey F, Graf R, Poncet N, and Camargo SM interpreted the data; Hagen CM and Camargo SM wrote the manuscript; all authors approved of the final version of the article.

Supported by Swiss National Science Foundation, Grant No. 31_166430/1 (to Verrey F).

Institutional review board statement: The study was reviewed and approved by Professors François Verrey and Rolf Graf.

Institutional animal care and use committee statement: Animal experiments adhered to the internationally accepted principles for the care and use of laboratory animals (License ZH075/15, Zurich Cantonal Veterinary office, Switzerland).

Conflict-of-interest statement: The authors have nothing to disclose.

Data sharing statement: No additional data are available.

ARRIVE guidelines statement: The authors have read the ARRIVE guidelines, and the manuscript was prepared and revised according to the ARRIVE guidelines.

Country/Territory of origin: Switzerland

ORCID number: Cristina M Hagen 0000-0002-0393-4154; Eva Roth 0000-0001-9707-1355; Theresia Reding Graf 0000-0003-4613-0874; François Verrey 0000-0003-3250-9824; Rolf Graf 0000-0001-7449-7302; Anurag Gupta 0000-0001-6850-3489; Giovanni Pellegrini 0000-0001-9593-5578; Nadège Poncet 0000-0002-0199-994X; Simone Mafalda Rodrigues Camargo 0000-0003-0091-7380.

S-Editor: Wu YXJ
L-Editor: A
P-Editor: Yu HG

REFERENCES

1 **Peery AF**, Crockett SD, Murphy CC, Jensen ET, Kim HP, Egberg MD, Lund JL, Moon AM, Pate V, Barnes EL, Schlusser CL, Baron TH, Shaheen NJ, Sandler RS. Burden and Cost of Gastrointestinal, Liver, and Pancreatic Diseases in the United States: Update 2021. *Gastroenterology* 2021 [PMID: 34678215 DOI: 10.1053/j.gastro.2021.10.017]
2 **Lankisch PG**, Apte M, Banks PA. Acute pancreatitis. *Lancet* 2015; **386**: 85-96 [PMID: 25616312 DOI: 10.1016/S0140-6736(14)60649-8]
3 **Nøjgaard C**, Becker U, Matzen P, Andersen JR, Holst C, Bendtsen F. Progression from acute to chronic pancreatitis: prognostic factors, mortality, and natural course. *Pancreas* 2011; **40**: 1195-1200 [PMID: 21926938 DOI: 10.1097/MPA.0b013e318221f569]
4 **Hu JX**, Zhao CF, Chen WB, Liu QC, Li QW, Lin YY, Gao F. Pancreatic cancer: A review of epidemiology, trend, and risk factors. *World J Gastroenterol* 2021; **27**: 4298-4321 [PMID: 34366606 DOI: 10.3748/wjg.v27.i27.4298]
5 **Wang GJ**, Gao CF, Wei D, Wang C, Ding SQ. Acute pancreatitis: etiology and common pathogenesis. *World J Gastroenterol* 2009; **15**: 1427-1430 [PMID: 19322914 DOI: 10.3748/wjg.15.1427]
6 **Zheng Z**, Ding YX, Qu YX, Cao F, Li F. A narrative review of acute pancreatitis and its diagnosis, pathogenetic mechanism, and management. *Ann Transl Med* 2021; **9**: 69 [PMID: 33553362 DOI: 10.21037/atm-20-4802]
7 **Peng C**, Li Z, Yu X. The Role of Pancreatic Infiltrating Innate Immune Cells in Acute Pancreatitis. *Int J Med Sci* 2021; **18**: 534-545 [PMID: 33390823 DOI: 10.7150/ijms.51618]
8 **Murtaugh LC**, Keefe MD. Regeneration and repair of the exocrine pancreas. *Annu Rev Physiol* 2015; **77**: 229-249 [PMID: 25386992 DOI: 10.1146/annurev-physiol-021014-071727]
9 **Hoang CQ**, Hale MA, Azevedo-Pouly AC, Elsässer HP, Deering TG, Willet SG, Pan FC, Magnuson MA, Wright CV, Swift GH, MacDonald RJ. Transcriptional Maintenance of Pancreatic Acinar Identity, Differentiation, and Homeostasis by PTF1A. *Mol Cell Biol* 2016; **36**: 3033-3047 [PMID: 27697859 DOI: 10.1128/MCB.00358-16]
10 **Giroux V**, Rustgi AK. Metaplasia: tissue injury adaptation and a precursor to the dysplasia-cancer sequence. *Nat Rev Cancer* 2017; **17**: 594-604 [PMID: 28860646 DOI: 10.1038/nrc.2017.68]
11 **Danielsson A**, Pontén F, Fagerberg L, Hallström BM, Schwenk JM, Uhlén M, Korsgren O, Lindskog C. The human

pancreas proteome defined by transcriptomics and antibody-based profiling. *PLoS One* 2014; **9**: e115421 [PMID: 25546435 DOI: 10.1371/journal.pone.0115421]

12 **Sans MD**, Tashiro M, Vogel NL, Kimball SR, D'Alecy LG, Williams JA. Leucine activates pancreatic translational machinery in rats and mice through mTOR independently of CCK and insulin. *J Nutr* 2006; **136**: 1792-1799 [PMID: 16772439 DOI: 10.1093/jn/136.7.1792]

13 **Hashimoto N**, Hara H. Dietary amino acids promote pancreatic protease synthesis at the translation stage in rats. *J Nutr* 2003; **133**: 3052-3057 [PMID: 14519783 DOI: 10.1093/jn/133.10.3052]

14 **Guo L**, Liu B, Zheng C, Bai H, Ren H, Yao J, Xu X. Inhibitory effect of high leucine concentration on α-amylase secretion by pancreatic acinar cells: possible key factor of proteasome. *Biosci Rep* 2018; **38** [PMID: 30361293 DOI: 10.1042/BSR20181455]

15 **Willet SG**, Lewis MA, Miao ZF, Liu D, Radyk MD, Cunningham RL, Burclaff J, Sibbel G, Lo HG, Blanc V, Davidson NO, Wang ZN, Mills JC. Regenerative proliferation of differentiated cells by mTORC1-dependent paligenosis. *EMBO J* 2018; **37** [PMID: 29467218 DOI: 10.15252/embj.201798311]

16 **Araya S**, Kuster E, Gluch D, Mariotta L, Lutz C, Reding TV, Graf R, Verrey F, Camargo SMR. Exocrine pancreas glutamate secretion help to sustain enterocyte nutritional needs under protein restriction. *Am J Physiol Gastrointest Liver Physiol* 2018; **314**: G517-G536 [PMID: 29167114 DOI: 10.1152/ajpgi.00135.2017]

17 **Rooman I**, Lutz C, Pinho AV, Huggel K, Reding T, Lahoutte T, Verrey F, Graf R, Camargo SM. Amino acid transporters expression in acinar cells is changed during acute pancreatitis. *Pancreatology* 2013; **13**: 475-485 [PMID: 24075511 DOI: 10.1016/j.pan.2013.06.006]

18 **Mackenzie B**, Erickson JD. Sodium-coupled neutral amino acid (System N/A) transporters of the SLC38 gene family. *Pflugers Arch* 2004; **447**: 784-795 [PMID: 12845534 DOI: 10.1007/s00424-003-1117-9]

19 **Fairweather SJ**, Shah N, Bröer S. Heteromeric Solute Carriers: Function, Structure, Pathology and Pharmacology. *Adv Exp Med Biol* 2021; **21**: 13-127 [PMID: 33052588 DOI: 10.1007/5584_2020_584]

20 **Pinho AV**, Rooman I, Reichert M, De Medts N, Bouwens L, Rustgi AK, Real FX. Adult pancreatic acinar cells dedifferentiate to an embryonic progenitor phenotype with concomitant activation of a senescence programme that is present in chronic pancreatitis. *Gut* 2011; **60**: 958-966 [PMID: 21193456 DOI: 10.1136/gut.2010.225920]

21 **Mastroberardino L**, Spindler B, Pfeiffer R, Skelly PJ, Loffing J, Shoemaker CB, Verrey F. Amino-acid transport by heterodimers of 4F2hc/CD98 and members of a permease family. *Nature* 1998; **395**: 288-291 [PMID: 9751058 DOI: 10.1038/26246]

22 **Hayashi K**, Jutabha P, Endou H, Sagara H, Anzai N. LAT1 is a critical transporter of essential amino acids for immune reactions in activated human T cells. *J Immunol* 2013; **191**: 4080-4085 [PMID: 24038088 DOI: 10.4049/jimmunol.1300923]

23 **Poncet N**, Halley PA, Lipina C, Gierliński M, Dady A, Singer GA, Febrer M, Shi YB, Yamaguchi TP, Taylor PM, Storey KG. Wnt regulates amino acid transporter Slc7a5 and so constrains the integrated stress response in mouse embryos. *EMBO Rep* 2020; **21**: e48469 [PMID: 31789450 DOI: 10.15252/embr.201948469]

24 **Häfliger P**, Charles RP. The L-Type Amino Acid Transporter LAT1-An Emerging Target in Cancer. *Int J Mol Sci* 2019; **20** [PMID: 31100853 DOI: 10.3390/ijms20102428]

25 **Nicklin P**, Bergman P, Zhang B, Triantafellow E, Wang H, Nyfeler B, Yang H, Hild M, Kung C, Wilson C, Myer VE, MacKeigan JP, Porter JA, Wang YK, Cantley LC, Finan PM, Murphy LO. Bidirectional transport of amino acids regulates mTOR and autophagy. *Cell* 2009; **136**: 521-534 [PMID: 19203585 DOI: 10.1016/j.cell.2008.11.044]

26 **Yanagisawa N**, Ichinoe M, Mikami T, Nakada N, Hana K, Koizumi W, Endou H, Okayasu I. High expression of L-type amino acid transporter 1 (LAT1) predicts poor prognosis in pancreatic ductal adenocarcinomas. *J Clin Pathol* 2012; **65**: 1019-1023 [PMID: 22813728 DOI: 10.1136/jclinpath-2012-200826]

27 **Quan L**, Ohgaki R, Hara S, Okuda S, Wei L, Okanishi H, Nagamori S, Endou H, Kanai Y. Amino acid transporter LAT1 in tumor-associated vascular endothelium promotes angiogenesis by regulating cell proliferation and VEGF-A-dependent mTORC1 activation. *J Exp Clin Cancer Res* 2020; **39**: 266 [PMID: 33256804 DOI: 10.1186/s13046-020-01762-0]

28 **Ventura A**, Kirsch DG, McLaughlin ME, Tuveson DA, Grimm J, Lintault L, Newman J, Reczek EE, Weissleder R, Jacks T. Restoration of p53 function leads to tumour regression in vivo. *Nature* 2007; **445**: 661-665 [PMID: 17251932 DOI: 10.1038/nature05541]

29 **Poncet N**, Mitchell FE, Ibrahim AF, McGuire VA, English G, Arthur JS, Shi YB, Taylor PM. The catalytic subunit of the system L1 amino acid transporter (slc7a5) facilitates nutrient signalling in mouse skeletal muscle. *PLoS One* 2014; **9**: e89547 [PMID: 24586861 DOI: 10.1371/journal.pone.0089547]

30 **Moret C**, Dave MH, Schulz N, Jiang JX, Verrey F, Wagner CA. Regulation of renal amino acid transporters during metabolic acidosis. *Am J Physiol Renal Physiol* 2007; **292**: F555-F566 [PMID: 17003226 DOI: 10.1152/ajprenal.00113.2006]

31 **Lyck R**, Ruderisch N, Moll AG, Steiner O, Cohen CD, Engelhardt B, Makrides V, Verrey F. Culture-induced changes in blood-brain barrier transcriptome: implications for amino-acid transporters in vivo. *J Cereb Blood Flow Metab* 2009; **29**: 1491-1502 [PMID: 19491922 DOI: 10.1038/jcbfm.2009.72]

32 **Yen LH**, Madhav B. Quantitating Inflammation in A Mouse Model of Acute Pancreatitis. *Pancreapedia* 2012 [DOI: 10.3998/panc.2012.2]

33 **Huang W**, Cane MC, Mukherjee R, Szatmary P, Zhang X, Elliott V, Ouyang Y, Chvanov M, Latawiec D, Wen L, Booth DM, Haynes AC, Petersen OH, Tepikin AV, Criddle DN, Sutton R. Caffeine protects against experimental acute pancreatitis by inhibition of inositol 1,4,5-trisphosphate receptor-mediated Ca2+ release. *Gut* 2017; **66**: 301-313 [PMID: 26642860 DOI: 10.1136/gutjnl-2015-309363]

34 **Lardon J**, Bouwens L. Metaplasia in the pancreas. *Differentiation* 2005; **73**: 278-286 [PMID: 16138828 DOI: 10.1111/j.1432-0436.2005.00030.x]

35 **Sakikubo M**, Furuyama K, Horiguchi M, Hosokawa S, Aoyama Y, Tsuboi K, Goto T, Hirata K, Masui T, Dor Y, Fujiyama T, Hoshino M, Uemoto S, Kawaguchi Y. Ptf1a inactivation in adult pancreatic acinar cells causes apoptosis through activation of the endoplasmic reticulum stress pathway. *Sci Rep* 2018; **8**: 15812 [PMID: 30361559 DOI:

10.1038/s41598-018-34093-4]
36 **Aguilar-Medina M**, Avendaño-Félix M, Lizárraga-Verdugo E, Bermúdez M, Romero-Quintana JG, Ramos-Payan R, Ruíz-García E, López-Camarillo C. SOX9 Stem-Cell Factor: Clinical and Functional Relevance in Cancer. *J Oncol* 2019; **2019**: 6754040 [PMID: 31057614 DOI: 10.1155/2019/6754040]
37 **Schlesinger Y**, Yosefov-Levi O, Kolodkin-Gal D, Granit RZ, Peters L, Kalifa R, Xia L, Nasereddin A, Shiff I, Amran O, Nevo Y, Elgavish S, Atlan K, Zamir G, Parnas O. Single-cell transcriptomes of pancreatic preinvasive lesions and cancer reveal acinar metaplastic cells' heterogeneity. *Nat Commun* 2020; **11**: 4516 [PMID: 32908137 DOI: 10.1038/s41467-020-18207-z]
38 **Hirota M**, Ohmuraya M, Hashimoto D, Suyama K, Sugita H, Ogawa M. Roles of Autophagy and Pancreatic Secretory Trypsin Inhibitor in Trypsinogen Activation in Acute Pancreatitis. *Pancreas* 2020; **49**: 493-497 [PMID: 32282761 DOI: 10.1097/MPA.0000000000001519]
39 **Halangk W**, Lerch MM, Brandt-Nedelev B, Roth W, Ruthenbuerger M, Reinheckel T, Domschke W, Lippert H, Peters C, Deussing J. Role of cathepsin B in intracellular trypsinogen activation and the onset of acute pancreatitis. *J Clin Invest* 2000; **106**: 773-781 [PMID: 10995788 DOI: 10.1172/JCI9411]
40 **Lyo V**, Cattaruzza F, Kim TN, Walker AW, Paulick M, Cox D, Cloyd J, Buxbaum J, Ostroff J, Bogyo M, Grady EF, Bunnett NW, Kirkwood KS. Active cathepsins B, L, and S in murine and human pancreatitis. *Am J Physiol Gastrointest Liver Physiol* 2012; **303**: G894-G903 [PMID: 22899821 DOI: 10.1152/ajpgi.00073.2012]
41 **Aghdassi AA**, John DS, Sendler M, Weiss FU, Reinheckel T, Mayerle J, Lerch MM. Cathepsin D regulates cathepsin B activation and disease severity predominantly in inflammatory cells during experimental pancreatitis. *J Biol Chem* 2018; **293**: 1018-1029 [PMID: 29229780 DOI: 10.1074/jbc.M117.814772]
42 **Machovich R**, Papp M, Fodor I. Protein synthesis in acute pancreatitis. *Biochem Med* 1970; **3**: 376-383 [PMID: 5523414 DOI: 10.1016/0006-2944(70)90004-9]
43 **Sans MD**, DiMagno MJ, D'Alecy LG, Williams JA. Caerulein-induced acute pancreatitis inhibits protein synthesis through effects on eIF2B and eIF4F. *Am J Physiol Gastrointest Liver Physiol* 2003; **285**: G517-G528 [PMID: 12773302 DOI: 10.1152/ajpgi.00540.2002]
44 **Saxton RA**, Sabatini DM. mTOR Signaling in Growth, Metabolism, and Disease. *Cell* 2017; **169**: 361-371 [PMID: 28388417 DOI: 10.1016/j.cell.2017.03.035]
45 **Krokowski D**, Han J, Saikia M, Majumder M, Yuan CL, Guan BJ, Bevilacqua E, Bussolati O, Bröer S, Arvan P, Tchórzewski M, Snider MD, Puchowicz M, Croniger CM, Kimball SR, Pan T, Koromilas AE, Kaufman RJ, Hatzoglou M. A self-defeating anabolic program leads to β-cell apoptosis in endoplasmic reticulum stress-induced diabetes *via* regulation of amino acid flux. *J Biol Chem* 2013; **288**: 17202-17213 [PMID: 23645676 DOI: 10.1074/jbc.M113.466920]
46 **Jiang P**, Mizushima N. LC3- and p62-based biochemical methods for the analysis of autophagy progression in mammalian cells. *Methods* 2015; **75**: 13-18 [PMID: 25484342 DOI: 10.1016/j.ymeth.2014.11.021]
47 **Sahani MH**, Itakura E, Mizushima N. Expression of the autophagy substrate SQSTM1/p62 is restored during prolonged starvation depending on transcriptional upregulation and autophagy-derived amino acids. *Autophagy* 2014; **10**: 431-441 [PMID: 24394643 DOI: 10.4161/auto.27344]
48 **Georgakilas AG**, Martin OA, Bonner WM. p21: A Two-Faced Genome Guardian. *Trends Mol Med* 2017; **23**: 310-319 [PMID: 28279624 DOI: 10.1016/j.molmed.2017.02.001]
49 **Giannandrea M**, Parks WC. Diverse functions of matrix metalloproteinases during fibrosis. *Dis Model Mech* 2014; **7**: 193-203 [PMID: 24713275 DOI: 10.1242/dmm.012062]
50 **Mailliard ME**, Stevens BR, Mann GE. Amino acid transport by small intestinal, hepatic, and pancreatic epithelia. *Gastroenterology* 1995; **108**: 888-910 [PMID: 7875494 DOI: 10.1016/0016-5085(95)90466-2]
51 **Salisbury TB**, Arthur S. The Regulation and Function of the L-Type Amino Acid Transporter 1 (LAT1) in Cancer. *Int J Mol Sci* 2018; **19** [PMID: 30103560 DOI: 10.3390/ijms19082373]
52 **Kantipudi S**, Fotiadis D. Yeast Cell-Based Transport Assay for the Functional Characterization of Human 4F2hc-LAT1 and -LAT2, and LAT1 and LAT2 Substrates and Inhibitors. *Front Mol Biosci* 2021; **8**: 676854 [PMID: 34124158 DOI: 10.3389/fmolb.2021.676854]
53 **Kurayama R**, Ito N, Nishibori Y, Fukuhara D, Akimoto Y, Higashihara E, Ishigaki Y, Sai Y, Miyamoto K, Endou H, Kanai Y, Yan K. Role of amino acid transporter LAT2 in the activation of mTORC1 pathway and the pathogenesis of crescentic glomerulonephritis. *Lab Invest* 2011; **91**: 992-1006 [PMID: 21403644 DOI: 10.1038/Labinvest.2011.43]
54 **Mehanna S**, Suzuki C, Shibata M, Sunabori T, Imanaka T, Araki K, Yamamura K, Uchiyama Y, Ohmuraya M. Cathepsin D in pancreatic acinar cells is implicated in cathepsin B and L degradation, but not in autophagic activity. *Biochem Biophys Res Commun* 2016; **469**: 405-411 [PMID: 26682926 DOI: 10.1016/j.bbrc.2015.12.002]
55 **Sendler M**, Maertin S, John D, Persike M, Weiss FU, Krüger B, Wartmann T, Wagh P, Halangk W, Schaschke N, Mayerle J, Lerch MM. Cathepsin B Activity Initiates Apoptosis *via* Digestive Protease Activation in Pancreatic Acinar Cells and Experimental Pancreatitis. *J Biol Chem* 2016; **291**: 14717-14731 [PMID: 27226576 DOI: 10.1074/jbc.M116.718999]
56 **Sendler M**, Dummer A, Weiss FU, Krüger B, Wartmann T, Scharffetter-Kochanek K, van Rooijen N, Malla SR, Aghdassi A, Halangk W, Lerch MM, Mayerle J. Tumour necrosis factor α secretion induces protease activation and acinar cell necrosis in acute experimental pancreatitis in mice. *Gut* 2013; **62**: 430-439 [PMID: 22490516 DOI: 10.1136/gutjnl-2011-300771]
57 **Sinclair LV**, Rolf J, Emslie E, Shi YB, Taylor PM, Cantrell DA. Control of amino-acid transport by antigen receptors coordinates the metabolic reprogramming essential for T cell differentiation. *Nat Immunol* 2013; **14**: 500-508 [PMID: 23525088 DOI: 10.1038/ni.2556]
58 **Yoon BR**, Oh YJ, Kang SW, Lee EB, Lee WW. Role of SLC7A5 in Metabolic Reprogramming of Human Monocyte/Macrophage Immune Responses. *Front Immunol* 2018; **9**: 53 [PMID: 29422900 DOI: 10.3389/fimmu.2018.00053]
59 **Crozier SJ**, Sans MD, Guo L, D'Alecy LG, Williams JA. Activation of the mTOR signalling pathway is required for pancreatic growth in protease-inhibitor-fed mice. *J Physiol* 2006; **573**: 775-786 [PMID: 16613881 DOI: 10.1113/jphysiol.2006.106914]

60 **Guo L**, Tian H, Shen J, Zheng C, Liu S, Cao Y, Cai C, Yao J. Phenylalanine regulates initiation of digestive enzyme mRNA translation in pancreatic acinar cells and tissue segments in dairy calves. *Biosci Rep* 2018; **38** [PMID: 29263147 DOI: 10.1042/BSR20171189]

61 **Ozaki K**, Yamada T, Horie T, Ishizaki A, Hiraiwa M, Iezaki T, Park G, Fukasawa K, Kamada H, Tokumura K, Motono M, Kaneda K, Ogawa K, Ochi H, Sato S, Kobayashi Y, Shi YB, Taylor PM, Hinoi E. The L-type amino acid transporter LAT1 inhibits osteoclastogenesis and maintains bone homeostasis through the mTORC1 pathway. *Sci Signal* 2019; **12** [PMID: 31289211 DOI: 10.1126/scisignal.aaw3921]

62 **Baar EL**, Carbajal KA, Ong IM, Lamming DW. Sex- and tissue-specific changes in mTOR signaling with age in C57BL/6J mice. *Aging Cell* 2016; **15**: 155-166 [PMID: 26695882 DOI: 10.1111/acel.12425]

63 **Gukovsky I**, Pandol SJ, Mareninova OA, Shalbueva N, Jia W, Gukovskaya AS. Impaired autophagy and organellar dysfunction in pancreatitis. *J Gastroenterol Hepatol* 2012; **27** Suppl 2: 27-32 [PMID: 22320913 DOI: 10.1111/j.1440-1746.2011.07004.x]

64 **Komatsu M**, Kageyama S, Ichimura Y. p62/SQSTM1/A170: physiology and pathology. *Pharmacol Res* 2012; **66**: 457-462 [PMID: 22841931 DOI: 10.1016/j.phrs.2012.07.004]

65 **Katsuragi Y**, Ichimura Y, Komatsu M. p62/SQSTM1 functions as a signaling hub and an autophagy adaptor. *FEBS J* 2015; **282**: 4672-4678 [PMID: 26432171 DOI: 10.1111/febs.13540]

66 **Zhao L**, Wang B, Gomez NA, de Avila JM, Zhu MJ, Du M. Even a low dose of tamoxifen profoundly induces adipose tissue browning in female mice. *Int J Obes (Lond)* 2020; **44**: 226-234 [PMID: 30705393 DOI: 10.1038/s41366-019-0330-3]

67 **Lakananurak N**, Gramlich L. Nutrition management in acute pancreatitis: Clinical practice consideration. *World J Clin Cases* 2020; **8**: 1561-1573 [PMID: 32432134 DOI: 10.12998/wjcc.v8.i9.1561]

68 **Pin CL**, Rukstalis JM, Johnson C, Konieczny SF. The bHLH transcription factor Mist1 is required to maintain exocrine pancreas cell organization and acinar cell identity. *J Cell Biol* 2001; **155**: 519-530 [PMID: 11696558 DOI: 10.1083/jcb.200105060]

69 **Huang W**, de la Iglesia-García D, Baston-Rey I, Calviño-Suarez C, Lariño-Noia J, Iglesias-Garcia J, Shi N, Zhang X, Cai W, Deng L, Moore D, Singh VK, Xia Q, Windsor JA, Domínguez-Muñoz JE, Sutton R. Exocrine Pancreatic Insufficiency Following Acute Pancreatitis: Systematic Review and Meta-Analysis. *Dig Dis Sci* 2019; **64**: 1985-2005 [PMID: 31161524 DOI: 10.1007/s10620-019-05568-9]

70 **Masui T**, Swift GH, Deering T, Shen C, Coats WS, Long Q, Elsässer HP, Magnuson MA, MacDonald RJ. Replacement of Rbpj with Rbpjl in the PTF1 complex controls the final maturation of pancreatic acinar cells. *Gastroenterology* 2010; **139**: 270-280 [PMID: 20398665 DOI: 10.1053/j.gastro.2010.04.003]

71 **Kim J**, Okamoto H, Huang Z, Anguiano G, Chen S, Liu Q, Cavino K, Xin Y, Na E, Hamid R, Lee J, Zambrowicz B, Unger R, Murphy AJ, Xu Y, Yancopoulos GD, Li WH, Gromada J. Amino Acid Transporter Slc38a5 Controls Glucagon Receptor Inhibition-Induced Pancreatic α Cell Hyperplasia in Mice. *Cell Metab* 2017; **25**: 1348-1361.e8 [PMID: 28591637 DOI: 10.1016/j.cmet.2017.05.006]

72 **Habib E**, Linher-Melville K, Lin HX, Singh G. Expression of xCT and activity of system xc(-) are regulated by NRF2 in human breast cancer cells in response to oxidative stress. *Redox Biol* 2015; **5**: 33-42 [PMID: 25827424 DOI: 10.1016/j.redox.2015.03.003]

73 **Menchini RJ**, Chaudhry FA. Multifaceted regulation of the system A transporter Slc38a2 suggests nanoscale regulation of amino acid metabolism and cellular signaling. *Neuropharmacology* 2019; **161**: 107789 [PMID: 31574264 DOI: 10.1016/j.neuropharm.2019.107789]

74 **Cheung AS**, de Rooy C, Levinger I, Rana K, Clarke MV, How JM, Garnham A, McLean C, Zajac JD, Davey RA, Grossmann M. Actin alpha cardiac muscle 1 gene expression is upregulated in the skeletal muscle of men undergoing androgen deprivation therapy for prostate cancer. *J Steroid Biochem Mol Biol* 2017; **174**: 56-64 [PMID: 28756295 DOI: 10.1016/j.jsbmb.2017.07.029]

75 **Della Torre S**, Mitro N, Meda C, Lolli F, Pedretti S, Barcella M, Ottobrini L, Metzger D, Caruso D, Maggi A. Short-Term Fasting Reveals Amino Acid Metabolism as a Major Sex-Discriminating Factor in the Liver. *Cell Metab* 2018; **28**: 256-267.e5 [PMID: 29909969 DOI: 10.1016/j.cmet.2018.05.021]

76 **Grabliauskaite K**, Hehl AB, Seleznik GM, Saponara E, Schlesinger K, Zuellig RA, Dittmann A, Bain M, Reding T, Sonda S, Graf R. p21(WAF1) (/Cip1) limits senescence and acinar-to-ductal metaplasia formation during pancreatitis. *J Pathol* 2015; **235**: 502-514 [PMID: 25212177 DOI: 10.1002/path.4440]

77 **Megyesi J**, Tarcsafalvi A, Li S, Hodeify R, Seng NS, Portilla D, Price PM. Increased expression of p21WAF1/CIP1 in kidney proximal tubules mediates fibrosis. *Am J Physiol Renal Physiol* 2015; **308**: F122-F130 [PMID: 25428126 DOI: 10.1152/ajprenal.00489.2014]

78 **Grabliauskaite K**, Saponara E, Reding T, Bombardo M, Seleznik GM, Malagola E, Zabel A, Faso C, Sonda S, Graf R. Inactivation of TGFβ receptor II signalling in pancreatic epithelial cells promotes acinar cell proliferation, acinar-to-ductal metaplasia and fibrosis during pancreatitis. *J Pathol* 2016; **238**: 434-445 [PMID: 26510396 DOI: 10.1002/path.4666]

79 **Yeo D**, Phillips P, Baldwin GS, He H, Nikfarjam M. Inhibition of group 1 p21-activated kinases suppresses pancreatic stellate cell activation and increases survival of mice with pancreatic cancer. *Int J Cancer* 2017; **140**: 2101-2111 [PMID: 28109008 DOI: 10.1002/ijc.30615]

80 **Kandikattu HK**, Venkateshaiah SU, Mishra A. Chronic Pancreatitis and the Development of Pancreatic Cancer. *Endocr Metab Immune Disord Drug Targets* 2020; **20**: 1182-1210 [PMID: 32324526 DOI: 10.2174/1871530320666200423095700]

81 **Cortes E**, Lachowski D, Rice A, Thorpe SD, Robinson B, Yeldag G, Lee DA, Ghemtio L, Rombouts K, Del Río Hernández AE. Tamoxifen mechanically deactivates hepatic stellate cells *via* the G protein-coupled estrogen receptor. *Oncogene* 2019; **38**: 2910-2922 [PMID: 30575816 DOI: 10.1038/s41388-018-0631-3]

82 **Cortes E**, Sarper M, Robinson B, Lachowski D, Chronopoulos A, Thorpe SD, Lee DA, Del Río Hernández AE. GPER is a mechanoregulator of pancreatic stellate cells and the tumor microenvironment. *EMBO Rep* 2019; **20** [PMID: 30538117 DOI: 10.15252/embr.201846556]

83 **Li X**, Clappier C, Kleiter I, Heuchel R. Tamoxifen affects chronic pancreatitis-related fibrogenesis in an experimental

mouse model: an effect beyond Cre recombination. *FEBS Open Bio* 2019; **9**: 1756-1768 [PMID: 31380604 DOI: 10.1002/2211-5463.12714]

84 **Wu J**, Zhang L, Shi J, He R, Yang W, Habtezion A, Niu N, Lu P, Xue J. Macrophage phenotypic switch orchestrates the inflammation and repair/regeneration following acute pancreatitis injury. *EBioMedicine* 2020; **58**: 102920 [PMID: 32739869 DOI: 10.1016/j.ebiom.2020.102920]

85 **Wang Q**, Wang H, Jing Q, Yang Y, Xue D, Hao C, Zhang W. Regulation of Pancreatic Fibrosis by Acinar Cell-Derived Exosomal miR-130a-3p *via* Targeting of Stellate Cell PPAR-γ. *J Inflamm Res* 2021; **14**: 461-477 [PMID: 33658824 DOI: 10.2147/JIR.S299298]

86 **Mauvais-Jarvis F**, Bairey Merz N, Barnes PJ, Brinton RD, Carrero JJ, DeMeo DL, De Vries GJ, Epperson CN, Govindan R, Klein SL, Lonardo A, Maki PM, McCullough LD, Regitz-Zagrosek V, Regensteiner JG, Rubin JB, Sandberg K, Suzuki A. Sex and gender: modifiers of health, disease, and medicine. *Lancet* 2020; **396**: 565-582 [PMID: 32828189 DOI: 10.1016/S0140-6736(20)31561-0]

87 **Shen HN**, Wang WC, Lu CL, Li CY. Effects of gender on severity, management and outcome in acute biliary pancreatitis. *PLoS One* 2013; **8**: e57504 [PMID: 23469006 DOI: 10.1371/journal.pone.0057504]

88 **Guleken Z**, Ozbeyli D, Acikel-Elmas M, Oktay S, Alev B, Sirvanci S, Velioglu Ogunc A, Kasimay Cakir O. The effect of estrogen receptor agonists on pancreaticobiliary duct ligation induced experimental acute pancreatitis. *J Physiol Pharmacol* 2017; **68**: 847-858 [PMID: 29550797]

Published by **Baishideng Publishing Group Inc**
7041 Koll Center Parkway, Suite 160, Pleasanton, CA 94566, USA
Telephone: +1-925-3991568
E-mail: bpgoffice@wjgnet.com
Help Desk: https://www.f6publishing.com/helpdesk
https://www.wjgnet.com